Design and Fabrication of Concentric Tube Robots: A Survey

Chibundo Nwafor¹, *Student Member, IEEE*, Cédric Girerd², Guillaume J. Laurent¹, Tania K. Morimoto^{2,3}, *Member, IEEE* and Kanty Rabenorosoa¹, *Member, IEEE*

Abstract—Concentric tube robots (CTRs) have drawn significant research attention over the years, particularly due to their applications in minimally invasive surgery (MIS). Indeed, their small size, flexibility, and high dexterity enable several potential benefits for MIS. Research has led to an increasing number of discoveries and scientific breakthroughs in CTR design, fabrication, control, and applications. Numerous prototypes have emerged from different research groups, each with their own design and specifications. This survey paper provides an overview of the state-of-the-art of the mechatronics aspects of CTRs, including approaches for the design and fabrication of the tubes, actuation unit, and end effector. In addition to the various hardware and associated fabrication methods, we propose to the research community, a unifying way of classifying CTRs based on their actuation unit architecture, as well as a set of specification details for evaluation of future CTR prototypes. Finally, we also aim to highlight the current advancements, challenges, and perspectives of CTR design and fabrication.

Index Terms—Concentric tube robots, robot design, surgical robotics, continuum robots.

I. Introduction

ONCENTRIC tube robots (CTRs) have become an important research topic, especially in the field of medical robotics, due to their many potential advantages in minimally invasive surgery (MIS). Compared to traditional open surgery, MIS involves reaching a surgical site through natural body orifices or small incisions, which can result in reduced patient discomfort, shorter recovery times, and improved surgical outcomes [1]–[5]. These benefits, along with the need for more dexterous, flexible, and miniaturized instruments for navigation in MIS procedures, have motivated the development of new minimally invasive surgical devices and robotic systems, including the development of continuum robots [6]. In particular, we focus here on the developments of a subclass of continuum robots, known as concentric tube robots, which have numerous potential advantages for MIS [7]–[11].

This work was supported by the regional BFC project CoErCIVe, the EIPHI Graduate School (contract "ANR-17-EURE-0002"), the ANR μ RoCS (contract "ANR-17-CE19-0005") and National Science Foundation (grant 1850400, and grant 2146095)

A. Concentric Tube Robots

CTRs are composed of a set of precurved, thin, hollow telescoping tubes, nested concentrically [12], [13]. Translation and rotation at the proximal end, causes the tubes to interact elastically with each other, leading to changes in the backbone configuration and distal tip pose [8], [14]-[16]. Just like other members of the continuum robot family, CTRs are not composed of discrete rigid links connected by joints and are instead characterized by their infinite-DOF, continuously bending and elastic structures [17], [18]. Due to the simplicity of their structure and their extrinsic actuation, they can be easily miniaturized [6] and are among the smallest type of continuum robot. In addition, their shape during deployment can be controlled along 3-D curves, without relying on or causing damage to body tissue [8]. They can also be easily deployed through fluid-filled channels or open cavities (e.g. blood vessels, air tracts etc) [4], [8]. The structural design of a CTR can be divided into three main parts: the tubes, the actuation unit, and the end effector, as shown in Fig. 1.

B. Prototypes

Over time, CTRs have advanced from manual instruments to automated systems. The first prototype, which dates back to around 1985, is composed of a straight outer tube with a precurved inner Nitinol wire. In 2005, a motorized CTR was introduced, and an initial patent was filed in 2014 [19]. Since then, CTRs have evolved tremendously, and many other patents related to CTRs have been filed, including ones for patient-specific customized designs [20], CTR actuation systems [21], a hybrid snake robot [22], a CTR for minimally invasive surgery [23], a bimanual neuroendoscopic robot [24], [25], an active cannula robotic system [26]-[29], a system for positioning and controlling concentric tube probes [29], [30], and a modular sterilizable robotic system for endonasal surgery [31]. Today, there are numerous CTR research groups around the globe, each continuously developing new prototypes, whose details can be found in the online CTR Prototype Resources https://cgirerd.github.io/ctr_prototyping_resources.html.

C. State of the Art

To date, a number of literature review/survey papers on CTRs have been written, each focusing on a specific aspect of the state-of-the-art. Webster et al. [17] focused on the design and relationship between the different modeling approaches

 $^{^1\}mathrm{Authors}$ are with SUPMICROTECH, CNRS, UFC, FEMTO-ST Institute, F-25000 Besançon, France. <code>rkanty@femto-st.fr</code> (corresponding author)

²Author is with the Department of Mechanical and Aerospace Engineering, University of California, San Diego, La Jolla, CA 92093 USA. cgirerd@eng.ucsd.edu

³Author is with the Department of Surgery, University of California, San Diego, La Jolla, CA 92093 USA. tkmorimoto@eng.ucsd.edu

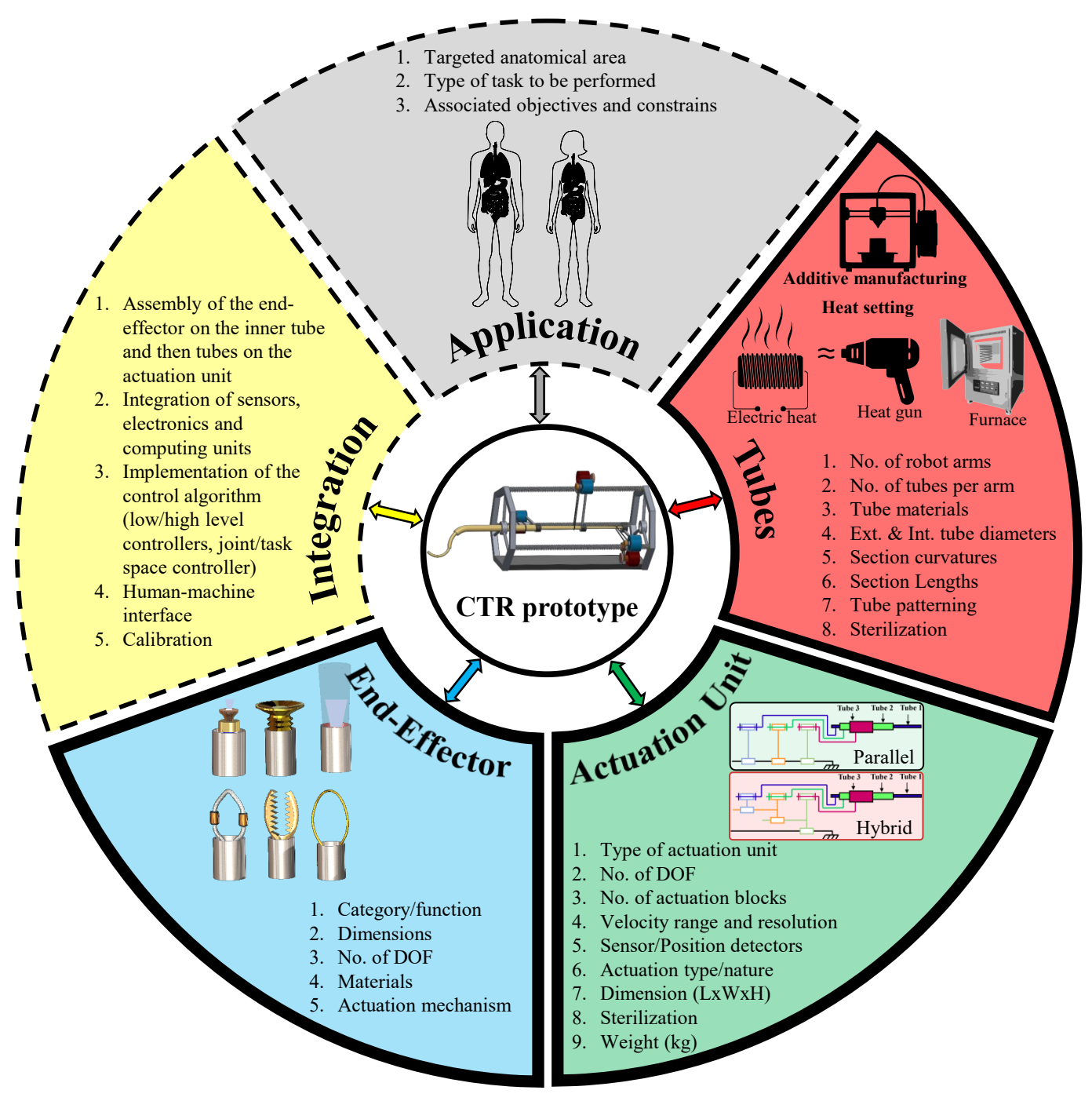


Fig. 1. The various components of a CTR prototyping, along with their respective specifications. The targeted application influences and determines the CTR design and its validation criteria. The CTR tubes are designed based on the geometry of the anatomical area and fabricated with processes that depend on the material selected. The actuation unit is also designed and fabricated using application and tube requirements. End effectors are selected and integrated into the innermost tube. An integration step consists in assembling all of these elements together, along with the implementation of a control system and validation of the CTR performance.

for constant curvature kinematics of continuum robots, for which CTRs are one example. Burgner-Kahrs et al. [6] covers continuum robots for medical interventions, with a broad overview on their different classifications, design, modeling, control and their detailed medical applications. The first review paper dedicated solely to CTRs discusses modeling, control, sensing, and design [14], and was later extended with more recent progress in modeling, control, motion planning, and

sensing [16]. Finally, Alfalahi et al. [4] and Mitros et al. [32], also address the generic design, modeling, and control of CTRs but with a major emphasis on their different clinical applications.

D. Contributions

While the mentioned reviews have focused on the robot modeling, control, sensing, planning, and proposed applications, none have addressed the design, fabrication approaches, and technologies of CTRs with significant detail. Therefore, this paper fills this gap by providing a review of the large variety of CTR designs and fabrication methods for all aspects of a physical prototype, including the tubes, actuation unit, and end effectors. Our contribution includes the creation of an online public resource that provides details on the tube designs and actuation units reported in the literature to date https://cgirerd.github.io/ctr_prototyping_resources.html. This resource will also be updated on a regular basis to include any new designs. We also propose a set of specification details, for future CTR prototype assessment and evaluation. This survey paper can serve as a resource to the research community with regards to various prototype designs in order to help find an avenue for creating a more mature robotic platform. The ultimate goal is to help channel major efforts towards other vital research challenges and to enable rapid improvements without requiring the development of new prototypes each time, which can be time consuming. Lastly, we also aim to classify the different concepts and approaches that have been developed and proposed by research groups, as well as to provide to the community a unifying way of classifying CTRs, which is based on the kinematics of the actuation unit. The remainder of the paper is organized as follows: Section II introduces the general CTR prototyping and specification. Section III-A presents the tube design, followed by the tube fabrication in Section III-B. Section IV describes the different actuation unit architecture and prototypes developed over the years, and Section V presents various CTR end effectors used for CTRs. A conclusion and discussion on the current state of the field and remaining challenges are proposed in Section VI.

II. SPECIFICATIONS AND PROTOTYPING

The general approach for CTR prototyping involves many design considerations and systematic steps to obtain the final desired robot. Despite the importance of the design specifications for reproducibility, evaluation, and progress towards a more mature CTR platform, often these details are left unreported in the literature, as illustrated by the incomplete/empty spaces in our online CTR Prototyping Resources https://cgirerd.github.io/ctr_prototyping_resources.html.

We propose to the research community, a unifying template of critical CTR specification details to be provided for future CTR prototypes in Fig. 1, as well as present the different components for CTR prototyping. These components are shown as the different sections in Fig.1, along with numerous design consideration and specifications. The procedure for prototyping CTRs can either be done sequentially, or multiple components can be carried out concurrently for faster and more efficient design. These components for CTR prototyping include:

1) Application: The prototyping of CTRs often begins with identifying the application and related requirements (e.g. MRI compatibility, ability to control remotely, sterilizability, etc.). Fig. 1 shows that application requirements influence the design

of the CTR and dictate how the final CTR prototype must be validated. There are numerous proposed medical applications, which are detailed extensively in [4], [6].

- 2) CTR Tubes: This component of CTRs is the most discussed in the literature. The tube design process involves finding the desired/optimal tube properties/specifications for the given application and the use of pre-operative medical images. These design specifications include the number of CTR arms, number of tubes, and the curvatures, lengths, diameters, and materials of each tube. There are two main documented fabrication approaches: additive manufacturing and heat setting. The fabrication method can also include structural modifications of the tubes for improved stability. Fig. 1 illustrates the different approach for precurving CTR tubes in literature, along with the necessary specification details. Section III-A of the paper discusses the CTR tubes in detail.
- 3) Actuation Unit: CTR actuation involves the translation and rotation of the tubes relative to one another. Fig. 1 shows the two actuation unit architectures commonly used in the literature to date, along with the proposed specification details to be provided for future prototypes. The architectures and proposed classifications of actuation units are detailed in Section IV.
- 4) End Effector: End effectors are needed in order to functionalize CTRs for particular applications. Some popular end effectors, including micro grippers, coagulators, curettes, cameras, and lasers, are shown in Fig. 1. Depending on the medical application or task, end effectors may be used for tissue manipulation, suction, ablation, visualization, etc. The critical specification details to consider for the end effectors are shown in Fig. 1, and Section V presents the different CTR end effector prototypes proposed to date.
- 5) Integration: After designing and fabricating the CTR tubes, actuation unit, and end effector, the last step is to integrate these components together, along with the associated electronics and computing units for their control. The tube translation and orientation must then be calibrated, which can be a delicate process for the orientation since the torsional interactions and friction between tubes make it difficult to identify the plane of curvature of the tubes after their concentric assembly [33]. After calibration, the robot can be used with one of the many proposed control laws, which include openloop, closed-loop, or human-in-the-loop control approaches, in a model-based or model-free scheme. For human-in-the-loop approaches, an appropriate human-machine interface must be selected to enable intuitive teleoperation. For more robust and accurate control, there is often an integration of sensors which could be vision-based shape sensing [34], [35], fiber Bragg grating shape sensing [36], [37], magnetic/hall effect shape sensing [38], [39], or force sensing [40], [41], for example. One key step here is the implementation of control algorithms, which could involve integration of low level motor controllers, high level controllers, joint space controllers, or task space controllers, depending on the CTR design. Since the area of CTR control has been reviewed extensively in [14], [16], we did not extend this review to cover this aspect, and instead focus on the prototyping of CTRs.

III. TUBES

A. Tube Design

In this section, the design variables considered for CTRs and the approaches used to design the tubes are presented.

1) Kinematics and Design Variables: While the links of serial or hyper-redundant robots can be independently controlled due to actuated joints placed between them, the segments of CTRs cannot be independently controlled. Indeed, translating or rotating a distal segment of a CTR requires the innermost, longest tubes to be actuated. This changes the bending and torsional equilibrium of the preceding robot segments, leading to a change in the entire robot shape. Therefore, designing a tube set to perform a given task in a constrained environment is not intuitive to designers, and necessitates the use of simulations that rely on the kinematic models of these robots.

Three kinematic models from the literature have mainly been used to aid in the synthesis of CTR tubes. These models, in order of development time, include a dominant stiffness model, a torsionally-rigid model, and a torsionally-compliant model. The dominant stiffness model [42] is the simplest model developed for CTRs. It assumes that each tube of the robot is infinitely stiff compared to the tubes inside of it, so that the shape of the robot is dictated by the shape of the stiffest tube in each given link. Infinite torsional stiffness is also assumed in this model. This model was used in some early work on the synthesis of these robots [43], as well as in special cases where the assumptions of the model hold [44].

However, the assumptions generally do not hold as the ratio of relative bending stiffness between the tubes approaches one, leading to the development of a second model that includes bending interactions between tubes. This model has higher accuracy and became more widely used for synthesis approaches developed between 2011 and 2013 (see Table I). Compared to the dominant stiffness model, the torsionally rigid model adds little complexity and still remains an algebraic closedform model. For this reason, it has still been used in recent years as a first pass in the synthesis before being refined using a torsionally-compliant model [10], due to its computational tractability. It is still useful today for the synthesis of CTRs in which tubes are not subject to torsional interactions and for which the torsionally-rigid and compliant models give identical results for stable robots, which is the case for CTRs that deploy in a follow-the-leader (FTL) manner [45]–[47].

The limits of this model for tubes that experience torsional interactions were shown and led to the development of torsionally-compliant models [7] that take both the bending and torsional equilibriums between the tubes into account. Torsion was first modeled in straight sections of the tubes only [15], [48], and was generalized later to both the straight and curved sections [7], [8], [17], [49], [50]. These models are considered in the literature as the sweet spot in terms of modeling complexity and accuracy [14], compared to the simpler dominant-stiffness [42] or torsionally-rigid models discussed [8], [17], and more complex models recently developed, that take tube clearance and friction into account [51], [52]. We note that to date these more complex kinematic models that include the effects of tube clearance and friction have not

been used for CTR design optimization purposes. In addition to the three main models presented, a torsionally-compliant kinematic model that takes external loads into account [53] has been used in one tube design approach [54], discussed later in this section.

The variables that can be considered for the synthesis of CTRs are the ones that appear in the kinematic models used and are reported in Fig. 2. For the dominant stiffness model, the parameters include the tube number, lengths, and curvatures. The torsionally-rigid model adds the bending stiffnesses of the tubes, which depends on their inner and outer diameters, and on the Young's modulus of the material used. Finally, the torsionally-compliant model adds the torsional stiffness, which depends on the inner and outer diameters of the tubes, as well as on the shear modulus of the material used.

- 2) Tube Design Approaches: The tube synthesis is split into two different categories: (1) the synthesis of a tube set to obtain a desired robot shape for specific tasks, and (2) the synthesis of tubes in order to obtain desired mechanical properties via structural modifications.
- a) Optimization of a Tube Set: The tube set design approaches for CTRs, sorted by objective function, are reported in Table I. Despite a high number of design variables included in the kinematic models, as detailed in the previous section, it is visible in Table I that the methods developed so far only lead to the synthesis of a subset of design parameters, with the others being pre-selected. Indeed, the tube number for instance is defined beforehand in all approaches. In general, designers tend to use 3 tubes, which allows tip pose control with 6 DOF for fully actuated tubes. However, we note the use of 2 tubes is also a common choice, and very few researchers have investigated the use of 4 [13], [76], [77] or even 5 tubes [77]. In addition, the tube materials, inner diameters, and outer diameters are usually predefined, except in [54] where they are optimized, and in [55] where the tube diameters are optimized. The consequence of this choice is that both the bending and torsional stiffnesses of the tubes, which are important parameters that impact the robot shape, are thus predefined, therefore limiting the design space of CTRs. This choice is usually made to limit the complexity of the synthesis as well as the computation time. Also, with the exception of

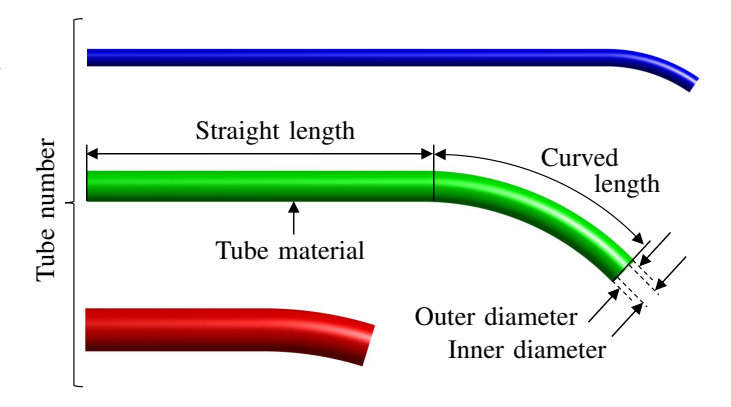


Fig. 2. Illustration of a set of CTR tubes, with their design variables represented.

a few approaches that investigate the benefits of tubes with continuously varying curvature along their lengths [62], [63], the tube curvatures are usually limited to constant curvature sections in the synthesis approaches [10]. Indeed, CTR tubes are usually considered to have a straight section, followed by a constant curvature section. This choice can be explained by kinematic models that are easier to implement under the constant curvature assumption, and for the ease of manufacturing of the tubes and identification of their curvature after their shape-setting. In addition, while all approaches listed in Table I except [62], [63] rely on constant-curvature tubes with two sections, such limitation still allowed researchers to tackle many applications and areas in the human body, as listed in Table I.

In addition to limiting the number of design variables and

tube shapes considered, CTR designers have also introduced various design guidelines in order to further simplify the synthesis problem. Bedell et al. proposed a decoupling of the robot in a navigation and a manipulation section [75], which was later integrated in the work of Bergeles et al. [10]. This decoupling has been reused in [78] for the search of feasible CTR shapes with a navigation and an exploration section. Bergeles et al. [10] further proposed that the stiffness of each link of the robot should dominate the stiffness of the previous ones, derived rules for approximate follow-the-leader deployment, and proposed the use of either fixed or varying curvature links for the robot, with the goal of simplifying the synthesis problem.

Diverse objective functions have been implemented for the synthesis of CTRs, and can be classified into two main cat-

TABLE I OVERVIEW OF THE SYNTHESIS APPROACH PROPOSED IN THE LITERATURE FOR CTRs, CLASSIFIED BY OBJECTIVE.

Maximize reachability, collision avoidance 2012 Sure et al. [56] ASA for tube design 1 motion planner (gradient-free) 2012 Baykal et al. [58] ASA for tube design 2015 Baykal et al. [58] ASA for tube design 2015 Baykal et al. [58] ASA for tube design 2015 Baykal et al. [58] ASA for tube design 2015 Baykal et al. [58] ASA for tube design 2015 Baykal et al. [58] ASA for tube design 2015 Baykal et al. [58] ASA for tube design 2015 Baykal et al. [58] ASA for tube design 2015 ASA for tube design 2016 A		ear Research	team	Optimization approach	Optimized p Tube length	arameters: Tube curv.	Kinematic model	Application	
Maximize reachability, collision avoidance 2017 Baykal et al. [58] (gradient-free))22 Lin et al.	[55]		✓	✓	TC	Laryngoscopy, Heart biopsy	
Maximize elastic stability, minimize tube lengths and curv., collision avoidance Maximize reachability, collision avoidance Stability Maximize reachability, collision avoidance Stability Maximize reachability, collision avoidance Stability Maximize field of view Maximize field of view Maximize elastic stability Maximize elastic stability Maximize elastic stability Maximize field of view Maximize elastic stability Maximize workspace, robot structural stiffness Maximize workspace, robot structural stiffness Maximize workspace, robot structural stiffness Maximize surface coverage Maximize surface coverage Maximize surface coverage Maximize surface coverage Maximize workspace, robot structural stiffness Maximize surface coverage Maximize surface coverage Maximize surface coverage Maximize surface coverage Maximize workspace, robot structural stiffness Maxim		017 Baykal et	al. [57]	+ motion planner	✓	✓	TC	Lung biopsy	
mize tube lengths and curv., collision avoidance Maximize reachability, collision avoidance, stability Maximize delastic stability Maximize elastic stability Maximize delastic stability Maximize of collaborative configurations between two CTRs Maximize workspace, robot structural stiffness Maximize surface coverage Maximize volume Maximize volume Maximize volume Maximize volume Maximize volume Maximize volume Maximize tobat Minimize robot Minimize far al. [67] Maximize tube lengths and curv., collision avoidance, stability Maximize al. [68] Brute force (gradient-free) Maximize delastic stability Maximize elastic stability Maximize elastic stability Maximize workspace, robot structural stiffness Maximize workspace, robot structural stiffness Maximize workspace, robot structural stiffness Maximize workspace, robot structural stiffness Maximize workspace, robot structural stiffness		O12 Torres et a	al. [59]		✓	✓	TC	Lung biopsy	
collision avoidance, stability 2017 Boushaki et al. [61] Pareto grid search (gradient-free)	engths and curv., col-)15 Bergeles e	et al. [10]	Nelder-Mead (gradient-free)	✓	√		Hydrocephalus treatment, cardiac surgery	
stability 2017 Boushaki et al. [61] Fracto grid search (gradient-free) \times TC Boe more free) Maximize field of view 2015 Hendrick et al. [44] Brute force (gradient-free) \times DS Pros Maximize elastic stability 2017 Ha et al. [62] Steepest descent (gradient-based) \times TC - Maximization of collaborative configurations between two CTRs 2018 Chikhaoui et al. [64]* Particle swarm (gradient-free) \times \times TC TC - Maximize workspace, robot structural stiffness 2019 Granna et al. [54] \dagger Particle swarm (gradient-free) \times \times TC with external loads - Maximize surface coverage 2016 Noh et al. [65] Nelder-Mead (gradient-free) \times TR Maliabla abla abla abla abla abla abla surgner-Kahrs et al. [68] Brute force, Greedy optimization (gradient-free) \times TR TR intra-evace from the following fraction (gradient-free) \times TR TR TR Skul abla abla abla abla abla abla abla ab		018 Girerd et	al. [60]	Brute force (gradient-free)	✓	✓	TC	Olfactory cleft biopsy	
Maximize elastic stability 2017 Ha et al. [62] Steepest descent (gradient-based) Maximization of collaborative configurations between two CTRs Chikhaoui et al. [64]* Particle swarm (gradient-free) Maximize workspace, robot structural stiffness 2018 Chikhaoui et al. [64]* Particle swarm (gradient-free) Maximize workspace, robot structural stiffness 2019 Granna et al. [54] † Particle swarm (gradient-free) Maximize surface coverage 2016 Noh et al. [65] Nelder-Mead (gradient-free) Maximize volume coverage 2017 Granna et al. [54], [66] Particle swarm (gradient-free) Maximize volume coverage 2018 Chikhaoui et al. [64]* Particle swarm (gradient-free) Maximize swarm (gradient-free) Maximize surface coverage 2016 Noh et al. [65] Nelder-Mead (gradient-free) Maximize volume coverage 2017 Granna et al. [67] Brute force, Greedy optimization (gradient-free) 2013 Burgner-Kahrs et al. [68] Brute force (gradient-free) 2013 Burgner-Kahrs et al. [69] Nelder-Mead (gradient-free) 2014 Burgner-Kahrs et al. [20] Nelder-Mead (gradient-free) Minimize robot Minimize robot Minimize robot	· · · · · · · · · · · · · · · · · · ·	017 Boushaki	et al. [61]			✓	TC	Deep anterior brain tu- mor surgery	
Maximize elastic stability 2014 Ha et al. [63] (gradient-based) Maximization of collaborative configurations between two CTRs 2018 Chikhaoui et al. [64]* Particle swarm (gradient-free) Maximize workspace, robot structural stiffness 2019 Granna et al. [54] † Particle swarm (gradient-free) Maximize surface coverage 2016 Noh et al. [65] Nelder-Mead (gradient-free) Maximize volume coverage 2017 Granna et al. [54], [66] Particle swarm (gradient-free) Maximize volume coverage 2017 Granna et al. [67] Brute force, Greedy optimization (gradient-free) Maximize volume coverage 2018 Chikhaoui et al. [64]* Particle swarm (gradient-free) Maximize surface coverage 2019 Granna et al. [65] Nelder-Mead (gradient-free) Maximize volume coverage 2017 Granna et al. [67] Brute force, Greedy optimization (gradient-free) Maximize volume coverage 2018 Durgner-Kahrs et al. [68] Brute force (gradient-free) Maximize volume coverage 2019 Burgner-Kahrs et al. [69] Nelder-Mead (gradient-free) Melder-Mead (gradient-free) Melder-Mead (gradient-free) Minimize robot Minimize robot	eld of view	15 Hendrick	et al. [44]	Brute force (gradient-free)		✓	DS	Prostate surgery	
Configurations between two CTRs 2018 Chikhaoui et al. [64]* Particle swarm (gradient-free) Maximize workspace, robot structural stiffness 2019 Granna et al. [54] † Particle swarm (gradient-free) Maximize surface coverage 2016 Noh et al. [65] Nelder-Mead (gradient-free) Maximize volume coverage 2017 Granna et al. [54], [66] Particle swarm (gradient-free) Maximize volume coverage 2017 Granna et al. [67] Brute force, Greedy optimization (gradient-free) 2013 Burgner-Kahrs et al. [68] Brute force (gradient-free) 2013 Burgner-Kahrs et al. [69] Nelder-Mead (gradient-free) Moscimize volume coverage 2018 Burgner-Kahrs et al. [69] Nelder-Mead (gradient-free) Moscimize volume coverage 2019 Farooq et al. [70] Nelder-Mead (gradient-free) Moscimize volume coverage Moscimize volume coverage Moscimize volume coverage 2017 Granna et al. [67] Brute force (gradient-free) Moscimize volume coverage Moscimize volume coverage 2018 Burgner-Kahrs et al. [68] Brute force (gradient-free) Moscimize volume coverage Moscimize volume Moscimize volume coverage Moscimize volume Moscimize	lastic stability					✓	TC	-	
Maximize workspace, robot structural stiffness 2019 Granna et al. [54] † Particle swarm (gradient-free) Maximize surface coverage 2016 Noh et al. [65] Nelder-Mead (gradient-free) TR Maliabla Maximize volume coverage 2017 Granna et al. [54], [66] Particle swarm (gradient-free) TR Maliabla 2017 Granna et al. [67] Brute force, Greedy optimization (gradient-free) 2013 Burgner-Kahrs et al. [68] Brute force (gradient-free) TR Intra evac 2013 Burgner-Kahrs et al. [69] Nelder-Mead (gradient-free) TR TR TR Skul Minimize robot Minimize robot Nelder-Mead (gradient-free) Nelder-Mead (grad		018 Chikhaoui	i et al. [64]*	Particle swarm (gradient-free)	✓	✓	TC	-	
Maximize volume coverage 2017 Granna et al. [54], [66] Particle swarm (gradient-free) 2017 Granna et al. [67] Brute force, Greedy optimization (gradient-free) 2013 Burgner-Kahrs et al. [68] Brute force (gradient-free) 2013 Burgner-Kahrs et al. [69] Nelder-Mead (gradient-free) 2014 Burgner-Kahrs et al. [2] Nelder-Mead (gradient-free) 2015 Farooq et al. [70] Nelder-Mead (gradient-free) Nelder-Mead (gradient-free)19 Granna et	al. [54] †	Particle swarm (gradient-free)	√	√	external	-	
Maximize volume coverage 2017 Granna et al. [54], [66] Particle swarm (gradient-free) 2017 Granna et al. [67] Brute force, Greedy optimization (gradient-free) 2013 Burgner-Kahrs et al. [68] Brute force (gradient-free) 2013 Burgner-Kahrs et al. [69] Nelder-Mead (gradient-free) 2014 TR TR Intra evac 2015 TR Pitti 2016 Farooq et al. [70] Nelder-Mead (gradient-free) Nelder-Mead (gr	urface coverage	Noh et al.	. [65]	Nelder-Mead (gradient-free)	✓	✓	TR		
Maximize volume coverage 2017 Granna et al. [67] tion (gradient-free) v TR Intra evac)17 Granna et	al. [54], [66]	Particle swarm (gradient-free)		✓	TR	Malignant brain tumors ablation	
Brute force (gradient-free) \checkmark TR 2013 Burgner-Kahrs et al. [68] Brute force (gradient-free) \checkmark TC Pitui 2013 Burgner-Kahrs et al. [69] Nelder-Mead (gradient-free) \checkmark TC Pitui 2011 Burgner-Kahrs et al. [2] Nelder-Mead (gradient-free) \checkmark TR Skul 2019 Farooq et al. [70] Nelder-Mead (gradient-free) \checkmark \checkmark TR Vitro Ligary Li		017 Granna et	al. [67]			✓	TR	Intracerebral hemorrhage evacuation	
2011 Burgner-Kahrs et al. [2] Nelder-Mead (gradient-free) \(TR \) Skul 2019 Farooq et al. [70] Nelder-Mead (gradient-free) \(\text{Vitr} \\ \text{Liga} \) Minimize robot 2016 Farooq et al. [71] Nelder-Mead (gradient-free) \(\text{Vitr} \\ \text{Liga} \))13 Burgner-K	Kahrs et al. [68]	Brute force (gradient-free)	✓	✓	TR		
Minimize robot 2019 Farooq et al. [70] Nelder-Mead (gradient-free) \checkmark - Vitro Liga		013 Burgner-K	Cahrs et al. [69]	Nelder-Mead (gradient-free)	✓	✓	TC	Pituitary gland surgery	
Minimize robot 2016 Farooq et.al [71] Nelder-Mead (gradient-free) Liga		011 Burgner-K	Xahrs et al. [2]	Nelder-Mead (gradient-free)	✓	✓	TR	Skull base surgery	
	Minimize robot distance to path			Nelder-Mead (gradient-free)	✓	✓	-	Vitroretinal surgery Ligation	
		017 Morimoto	et al. [73]	Analytical formulation	✓	✓	TR	Kidney stone removal	
	Minimize tube lengths and curvature, collision avoidance)11 Bedell et	al. [75]		√	✓	TR	Cardiac surgery	
collision avoidance 2011 Apor et al. [43] Generalized pattern search DS Hyd)11 Anor et al	1. [43]		✓	✓	DS	Hydrocephalus treatment	

^{*:} Method applied to a dual-arm robot

DS: Dominant stiffness

ASA: Adaptive simulated annealing (gradient-free) RRT: Rapidly-exploring random trees (gradient-free)

^{§:} Also includes optimization of tube inner and outer diameters

^{†:} Also includes optimization of tube inner and outer diameters and Young's modulus

TR: Torsionally-rigid TC: Torsionally-compliant

egories. The first category corresponds to objective functions related to the task to be performed, including mostly obstacle avoidance and reachability. The goal in these scenarios is to design a set of tubes to enable the robot tip to reach a desired pose in Cartesian space, or to sweep a given volume, as illustrated in particular in [2], [10], [68], [69], [75]. The second category corresponds to objective functions that constrain the design of the CTR or its joint values, in order to guide solvers towards a feasible robot. For instance, tube lengths and curvatures are usually minimized in order to avoid loopings of the robot in the anatomy [43], or to increase its stiffness or remain in the admissible stress limit of the material [75]. While not being an objective, constraints on the material strain have also been implemented in [55] to ensure tube mechanical integrity during usage. Researchers also sought to maximize the robot stability [10], [60]–[63] in order to avoid having multiple solutions to the direct kinematic model, which results in a snapping phenomena occurring due to the accumulated torsional energy releasing when they are actuated.

In addition, it should be noted that most work has focused on the synthesis of CTRs by assessing collisions for a fully deployed configuration only. While this ensures that the deployed robot meets the desired performance, it does not guarantee that the robot can deploy to the site of interest without colliding with the anatomy. In order to achieve a collision-free path, the synthesis of the CTR must be coupled to a motion planner in order to take the deployment of the robot into account. This approach has been explored in the work of Torres et al. [59], with an RRT (Rapidly-exploring Random Tree) to sample the design parameters and another RRT to sample the joint variables, Baykal et al. [57], [58], [79], with methods that enables the obtention of tube geometries as well as a motion plan, and more recently in Lin et al. [55].

Overall, it can be observed from Table I that all design algorithms proposed to date are gradient-free optimization approaches, except the recent work of Lin et al. [55]. Other exceptions are [62], [63], however these works did not consider task objectives and constraints. This trend can be attributed to the difficulties of formulating the kinematic model of CTRs in a way that is differentiable with respect to its design variables, since the robot shape is obtained by a boundary value problem followed by two integrations. It can also be explained by the variety of constraints, such as collisions with the anatomy, computed from triangular meshes that represent the areas of interest [10], and optimization objectives, such as volumes swept by the robot tip, computed using ratios of voxels [54], [66], that have been easier to integrate in gradient-free frameworks due to their formulations.

b) Modification of the Mechanical Properties of Tubes via material removal: While the approaches presented previously deal with the design of a set of tubes, each of them having an annular cross-section along their entire length, more recent research has investigated ways to modify the mechanical properties of the tubes, via structural modifications. These structural modification take the form of patterns where tube material is removed, as illustrated in Fig. 4. The geometry of the patterns enables independent modifications of the bending and torsional stiffnesses of the tubes, which are normally

related by the Poisson's ratio in the case of a uniform material along the radius and length of the tubes. The goal of using such patterns is to lower the bending to torsional stiffness ratio of CTR tubes in order to obtain stability for the robot and avoid any snapping phenomena during usage [84]-[86]. In particular, tube patterning has been investigated for use in follow-theleader deployment [87], [88], for which unstable robots must have their tubes patterned to obtain stability, while keeping a desired robot shape. In general, tube patterning approaches to date have included the use of helical tubes composed of multiple layers [89], patterned or cellular tubes [81], [82], [89], and patterns defined using topology optimization [83], [90], more particularly with rhombus patterns identified in [83]. Cases of helically-patterned Nitinol tubes for use as steerable needles have also been reported in the literature [91]. While the above approaches have focused on structural modification of tubes that affects their bending stiffness as uniformly as possible around their circumference, recent research has shown the advantages of patterning tubes to obtain direction-dependent flexural rigidity [92]. Indeed, it was shown that patterning planar, piecewise-constant curvature tubes in their curvature plane enables stability to be obtained more efficiently, while preserving most of the structural stiffness of the tubes, which is highly beneficial for tasks that require interactions between the robot and tissue, for instance.

Despite the advantages of tube patterning on CTR stability, it has been observed that translating and rotating patterned tubes relative to one another can be difficult, due to physical interference between their notches [81]. One solution adopted was to insert thin PTFE tubes between patterned tubes in order to isolate their notches. However, such tubes tend to wear after repetitive motions of the tubes and do not constitute a permanent solution [81]. In order to improve the CTR stability, another approach has been to decrease the tube wind-up along the transmission lengths by using a more torsionally rigid material compared to the material of the deployed portion of the tubes. For this purpose, researchers have combined stainless steel transmission lengths with deployed Nitinol tube lengths [93], [94].

3) Tube Design: Perspectives: With regards to the tube design, there are a number of improvements that can be made. First, the current synthesis approaches fail to take advantage of all design variables, as most of them are being preselected. Indeed, the tube inner and outer diameters, the tube materials, and number of constant-curvature sections, are usually predefined and thus not optimized. Yet, these parameters play an important role in the variety of shapes that a CTR can adopt. In addition, current tube geometries considered, usually composed of a straight section followed by a curved one, could be generalized to tubes with more than two sections or with continuously varying curvature along their lengths. However, such an increase in the number of design variables might not lead to tractable problems for the gradient-free algorithms used in the literature to date, and the community could benefit from the investigation of gradient-based approaches, such as in Lin et al. [55]. Although, optimizing variables such as tube materials and the number of tube sections is difficult in gradient-based approaches, since these variables take non-

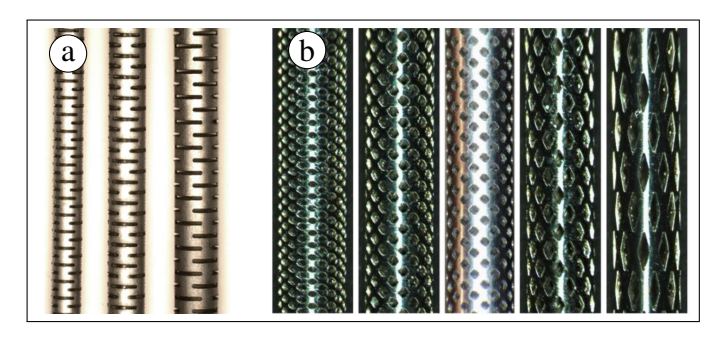


Fig. 4. Example of pattern shapes proposed by researchers, with (a) parameterised patterns simulated using FEA [82] ©[2015] IEEE and (b) diamond-shape patterns obtained using topology optimization [83] ©[2021] IEEE.

continuous values. Thus, there is a need for optimization approaches that can handle a large number of continuous and discontinuous design variables in order to push the boundaries of CTR tube design forward. Furthermore, more accurate kinematic models, that include the effects of tube clearance and friction between them [51], [52] could be included in the tube design algorithms in order to increase the shape fidelity representation of these robots. Including tube anisotropy in design approaches would also be of interest to extend the capabilities of CTRs. However, locally patterning tubes along their circumferences and lengths usually lead to non-uniform bending and torsional stiffnesses along these directions. As a result, translating and rotating such tubes could lead to tip pose oscillations, which have not been quantified in current research. The research community does not seem to have converged to a specific pattern, which means that additional work could be required in order to identify the most efficient pattern geometries. Tube design should also incorporate path planning, as in most recent approaches, in order to ensure a collision-free deployment of the robot to the target. Current planning is limited by the accuracy of the kinematic models, which neglect tube clearance and friction, leading to a 3-D shape of the robot which is, in practice, different from the predicted one. The use of more advanced kinematic models could lead to improved path planning and tube designs. In addition, CTR stability should also be included in the planning of these robots for tube synthesis purposes. Although current design approaches have led to tube sets capable of accessing

hard-to-reach areas of the human body, these approaches significantly reduce the overall design space, which could lead to sub-optimal results or failure to succeed in given scenarios.

B. Tube Fabrication

One critical aspect of CTR prototyping is the tube fabrication, which often depends on the material to be used. CTR tubes are primarily made using Nitinol, which is a superelastic alloy of nickel and titanium, and more recently, polymer materials have also been used [95]–[97]. A comparison of the mechanical properties of materials used to date are given in Table II, which can serve as a reference for choosing a tube material. This section presents the main CTR tube fabrication methods to date: heat-setting of Nitinol and heat-shrink plastic tubes, additive manufacturing for plastic tubes, and the fabrication of patterned tubes. Collections of the various tube prototypes in the literature are provided in our CTR Prototyping Resources https://cgirerd.github.io/ctr_prototyping_resources.html for both single and multi-arm robots.

1) Heat Setting:

a) Heat Setting of Nitinol Tubes: Nitinol tubes are typically sold as straight tubes by manufacturers (see [104]-[106] for lists of various manufacturers/suppliers). Nitinol is the predominantly used material for CTR tubes thanks to its large superelastic range, which enables large workspaces compared to CTRs made of other materials [80], [96]. There are several patents related to the shape setting of Nitinol, including patents for shape alloy treatment [107], drawing heated Nitinol followed by forming and rapid quenching [108], and treatment for cold worked Nitinol under non-stress induced shape setting [109]. Although some companies (e.g. Minitubes [110], Memry [111], Nimesis [112]) have mastered the shape setting of Nitinol using proprietary processes, obtaining these precurved tubes is typically expensive. The research community has therefore developed processes for bending commercially available straight tubes, typically using heat treatment approaches.

Heat treating depends on the state of the Nitinol acquired from the provider and requires considerable technical knowledge and specialized equipment in order to obtain an optimized, consistent, and accurate result without any unwanted

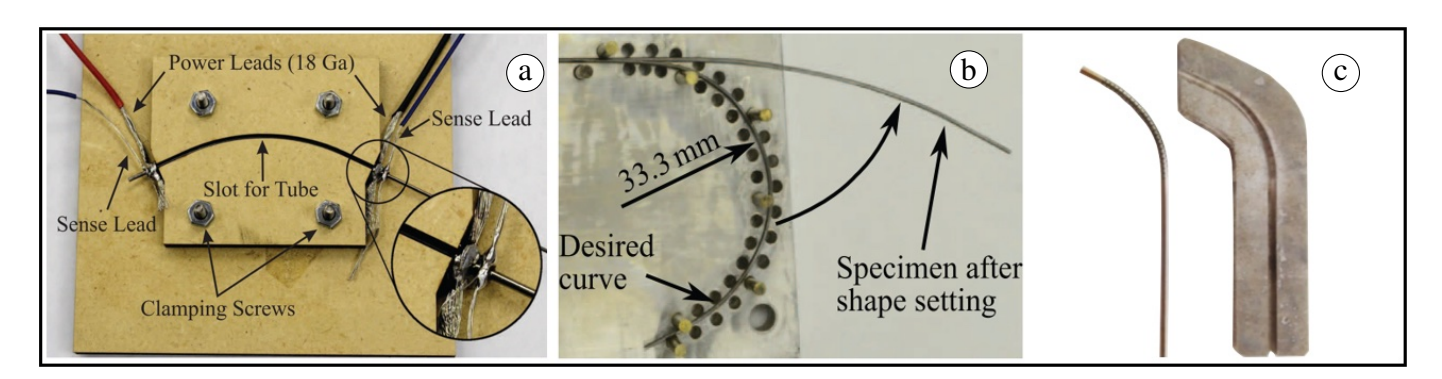


Fig. 3. a) Joule heating effect by high current flow through the tube [80] ©[2016] IEEE, b) Air furnace heat treatment using metal fixture with brass pins [80] ©[2016] IEEE, c) Air furnace annealing process using engraved aluminum mold [81] ©[2014] IEEE.

TABLE II
MECHANICAL COMPARISON OF THE DIFFERENT TUBE MATERIALS.

Property	Material	Rating	Remarks				
	Nitinol	****	Yield strength: 195 - 690 MPa and Young modulus: ~83 GPa [98], recoverable strain up to 11% [99]				
Elasticity and	PLA	***	Yield strength: 60 - 70 MPa and Young modulus: 2.5 - 7.8 GPa [96]				
recoverable	PCL	**	Yield strength: 16.1 MPa and Young modulus: 0.34 - 0.36 GPa [96]				
_	NYL	***	Yield strength: 60 - 70 MPa and Young modulus: 1.5 - 4 GPa [96], [97]				
	Heat-shrink tube	**	Tensile strength: 23 - 39.6 MPa and Young modulus: 0.44 - 0.64 GPa [65], [100]				
	Nitinol	****	1.49 mm [96]				
Tip repeatability	PLA	****	0.3 - 3.1 mm (the mean error = 1.7 mm) [96]				
error and	PCL	**	0.2 - 9.8 mm (the mean error = 5 mm) [96]				
Fatigue resistance	NYL	***	0.4 - 7.6 mm (the mean error = 4 mm) [96]				
	Heat-shrink tube	**	1.0 - 2.1 mm (the mean error = 1.55 mm) [101]				
Miniaturization and minimum PCL resolution NYL	Nitinol	*****	Min. internal/external diameter: 0.258/0.33 mm; min wall thickness 0.036mm [102]				
	PLA	***	Min. int./ext. diam: 0/1.2 mm, 0.6 wall thickness and resolution 100 microns [96]				
	PCL	***	Min. int./ext. diam: 0/1.2 mm, 0.6 wall thickness and resolution 100 microns [96]				
	NYL	***	Min. int./ext. diam: 0/1.2 mm, 0.6 wall thickness and resolution 100 microns [96]				
	Heat-shrink tube	****	Min. int./ext. diam: 1.17/1.67 mm, 0.5mm wall thickness [65]				
	Nitinol	****	11e-6/°C [98]				
Thermal	PLA	****	8.5e-5/°C [103]				
effect/shock (Expan. coeff.)	PCL	***	16e-5/°C [103] this can even reshape by heating in hot water [96]				
	NYL	****	5e-5/°C [103]				
	Heat-shrink tube	**	(8.3-10.5)e-5/°C [100]				
Surface friction/ smoothness	Nitinol	****	High surface smoothness (best)				
	PLA	**	Low surface smoothness (worst) [96]				
	PCL	***	Medium surface smoothness (good) [96]				
	NYL	****	Medium surface smoothness (best among 3-D printed polymers) [96]				
	Heat-shrink tube	***	Medium surface smoothness [65]				
Fabrication complexity/ customization	Nitinol	***	More complex and challenging fabrication process [95], [96]				
	PLA	****	Not rigorous and direct process [95], [96]				
	PCL	****	Not rigorous and direct process [95], [96]				
	NYL	****	Not rigorous and direct process [95], [96]				
	Heat-shrink tube	****	Simple and direct process [65], [101]				

^{*:} Symbol used for the ranking/grading, PLA: Polylactic, PCL: Polycaprolactone, NYL: Polyamide/Nylon

spring-back or material aging [80]. There are two main heat treatment methods for shape-setting Nitinol tubes: (1) heat diffusion using a furnace and (2) joule heating by passing current through the tubes. For both methods, a patterned fixture or mold with the desired shape engraved, is used to fix the shape of the initially straight tubes, as shown in Fig. 3. These processes require accurate timing and temperature in order to achieve the desired goal, and deviations can lead to relaxation of the tubes from the desired shape [68] or a loss of their superelastic properties.

For the furnace heat treatment approach, the use of a box/small furnace has been widely adopted due to cost, versatility, precise temperature control, uniform heat distribution and the ability to rapidly prototype without much risk [80], [113], [114], since most are equipped with advanced features, such as temperature control. Using this approach, groups have demonstrated the bending process by constraining the straight commercial Nitinol tubes in a variety of fixtures designed to have the desired precurved shape (see Fig. 3b. and Fig. 3c). Once constrained, the tubes were then heated in the furnace for 10 minutes at 500°C [113], [115]–[117] and finally quenched in water at room temperature to suppress the aging effect. The resulting tubes, however, had a high springback, and the quality of the results seemed difficult to predict. In addition, this process is said to be highly inefficient which

require several trials, significant time, energy and material, especially the cost of mold machining and use of thick steel to minimize buckling and thermal expansion bulge, which conversely absorb more heat than the tube itself. All these prompted the development of electric heat setting techniques.

Electric heating relies on joule heating, where electric current passing through the Nitinol tube (which acts as a resistance) generates the heat needed to shape the tube with the desired curvature [80], [113], [118]. The proposed setup includes temperature control and monitoring using real-time resistance measurements of the tube. This method was observed to have several advantages, including (i) the use of high current enables the shape setting temperature to be reached very quickly, and (ii) there is minimal equipment required to control the heating while supplying the required current. It should be noted that the fixture with an engraved pattern must be an electrical insulator with low thermal conductivity, which excludes the use of metals. A medium density fiberboard, ceramic or 3D printed mold has been used by researchers [80], [114] (see Fig. 3a) for this purpose. The cooling was done through natural convection, and it was observed that the system operates correctly even when considering the nonuniformity of the heat sinking effect. Finally, a comparison between the two heat setting methods showed that the electric heating technique results is more energy efficient with less

spring-back for the tubes compared to the furnace heating method, as well as faster shape-setting processes [80], [114], [119]. However, the drawbacks of electric heating are: (1) the requirement for a specific setup, which has some hardware limitations (2) tuning and calibrating the system to match the tube-specific transition temperature is challenging, and (3) the uneven thermal gradient/expansion along the tube can result in undesirable distorted shapes near the clamped ends [114]. Despite the high cost and inefficiency, the most commonly used approach is still the furnace heating technique, as recorded in 24 papers [35], [46], [62], [70], [81]–[83], [90], [120]–[135], as compared to the electric heating with only 6 papers [11], [114], [136]–[139], while both approaches are recorded in [80], [119], [140].

b) Heat Setting of Plastic Tubes: Although heat treatment has mostly been used for Nitinol tubes, recent work has investigated the use of heat-shrink tubes. This approach provides an alternative, rapid, and cost-effective fabrication method. Indeed, medical-grade heat-shrink tube HS-S14 (Insultab, Inc., Woburn, MA, USA) has been used in [65], [101] for the innermost tube of a three-tube CTR. The bending process consisted of placing the heat-shrink tube in a jig with a metallic guide wire inside its lumen to preserve its shape. The assembly was heated with a heat gun and quenched in water after shrinkage of the material with results as shown in Fig. 5. The benefits of using heat-shrink tubes include the low cost and simple process that does not require any expensive and specialized equipment, such as a furnace or electrical heat setting setup. In addition, heat-shrink tubes can be bent in a timely manner, allowing for the fast fabrication of patientand task-specific tube sets. Nevertheless, some limitations remain with this type of material. Indeed, the fabricated bent tubes had their radius of curvature permanently increased when translated inside a straight metal tube. More precisely, rapid changes in their radius of curvature occurred below a few dozen cycles, most likely due to fatigue [65], [101] and tended to stabilize afterwards. Presently, this approach seems to be discontinued, as it is limited to the fabrication of only the innermost CTR tube. However, there are many potential benefits of the approach, which could be worthwhile to explore.

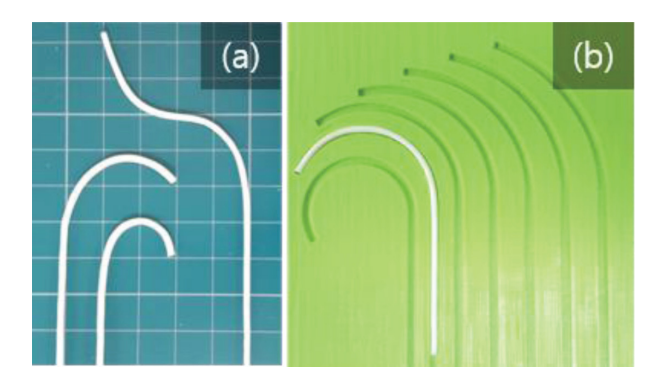


Fig. 5. (a) Fabricated heat-shrink plastic tubes and (b) the jig for fabrication of tubes, extracted from [65] ©[2016] IEEE.

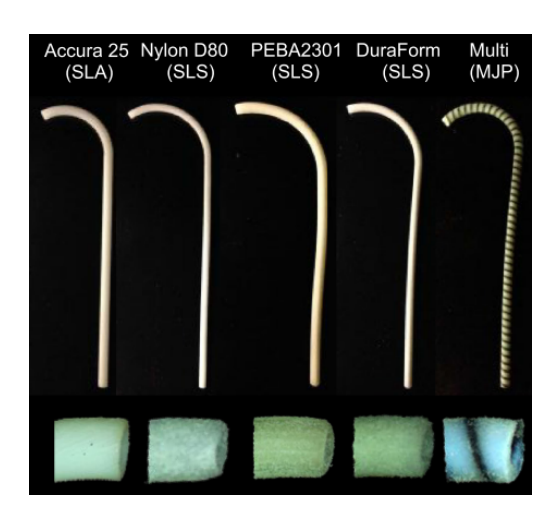


Fig. 6. CTR tube prototypes fabricated with additive manufacturing using different material and process. The stereolithography-SLA (for Accura 25). The selective laser sintering-SLS (for Nylon D80, PEBA 2301, and DuraForm). multijet printing-MJP (with different material) by Morimoto et al. [73] ©[2017] IEEE.

2) Additive Manufacturing for Plastic Tubes: Additive manufacturing has made it possible to transform a digital model into a physical 3-D object, and is now often used to create rapid prototypes in a number of industries. It has enabled personalized prototyping, where a given patient scan can be used to generate a personalized digital model, as can be seen in [73], [96]. Additive manufacturing is a layer-by-layer controlled process of creating physical objects using a digital model. There are many different technologies and materials available for additive manufacturing, and several were studied in the context of CTRs [95], each with their pros and cons. The first step for prototyping using additive manufacturing is to create a mesh file of the part to be printed. It was observed that the key to obtaining optimal results, depends heavily on the printer settings [96]. Once the print is complete, there may be additional post-processing steps to clean unwanted material, depending on the additive manufacturing process used.

The different materials that were investigated by Amanov et al. [96] lead to varying results. Sixteen tubes for each material were evaluated, and it was observed that Nylon and Polycaprolactone (PLC) had a comparable accuracy/tip position error range to that of Nitinol tubes and possess better properties (e.g. surface friction and stiffness/elasticity etc.) than Polylactic (PLA), with Nylon having the smoothest surface. Amanov et al. demonstrated that prototypes created using additive manufacturing can be fabricated quickly and can easily be patient-specific and made on site even in a hospital. Another extensive investigation of prototypes created using additive manufacturing, was carried out by Morimoto et al. with a focus on personalized designs for pediatric patients using ultrasound images. In [72], a PCL material was used and follow-the-leader deployment was implemented. In another paper [95], Morimoto et al. used several additive manufacturing processes and materials, as shown in Fig. 6, to investigate their different performances. It was observed that the combination of both SLS (using a polyether block amide) for the outer tube and stereolithography (polypropylene-like

material) for the inner tube, gave the required maximum strain combination although biocompatibility was not considered. The use of Multijet additive manufacturing (MJT) was later explored for printing Nylon-12 [97] and was found to have higher accuracy, finer resolution, and a smaller minimum wall thickness compared to SLS, which improved the result of the printed CTR tubes.

- 3) Fabrication of Patterned Tubes: Patterning tubes involves removing material from annular cross-section tubes. Although patterned tubes can be implemented with any of the materials cited previously for CTRs, they have mainly been explored for Nitinol, and fabrication techniques adapted to this material were explored. Various manufacturing techniques have been considered, including milling [141], laser cutting [82], electro discharge machining [142] and femtosecond laser machining [143]. Milling can lead to unintentional heat treatment of the material due to high temperatures during the process, and the diameters of the mill bits limit the dimensions of the notches that can be made on the tubes. Laser cutting with long pulse-widths can also generate significant heat, but allows for smaller patterns to be made. Electro discharge machining and femtosecond laser machining both enable small patterns to be made, with femtosecond laser machining being able to produce the smallest ones. Femtosecond laser machining also minimizes the heat-affected zones at the edges of the pattern, limiting the undesired heat-treatment of the material [143].
- 4) Tube Fabrication: Perspectives: Although both Nitinol and polymers have been used to create CTRs. Nitinol continues to be the most commonly used material. Plastic tubes gained some popularity due to their potential for being lowcost and enabling fast fabrication times. The apparent decline and lack of adoption of additive manufacturing for CTR tubes can likely be attributed to the present state of additive manufacturing technologies (printer resolution and obtainable material properties) and some of the comparable factors identified in Table II. However, Nitinol is an expensive material and involves complex processes for shape-setting. Currently, the research community has almost reached a stagnating point, with the challenge of constant use of Nitinol for CTR tube design and prototyping. To enable more efficient customization, improvements in miniaturization, lower-cost tubes, and rapid onsite fabrication, there is a need for complementary, alternative materials with viable properties.

IV. ACTUATION UNITS

Actuation units enable the conversion of energy into mechanical movement. For CTRs, the actuation is achieved by translating and rotating the tubes relative to one another [12], [13]. Their actuation unit is simply composed of a set of actuation block(s), where each block is individually connected to the proximal end of a tube and generates the desired translation and rotation to drive that tube, as shown in Fig. 7. Generally, the number of tubes to be deployed and the required DOF per tube determine the number of actuation blocks in an actuation unit. The total number of DOF of a CTR is usually given

as 2n, where n is the number of tubes and 2 corresponds to one DOF in rotation and 1 DOF in translation. Despite their importance, actuation units are often described in less detail in the literature compared to the tubes themselves, and often they appear in figures without technical specifications regarding their design and kinematic architecture.

Although the physical appearances of some actuation units have similarities, their internal architectures may differ. Rather than using the various nomenclatures in the literature e.g. multi-arm, MRI-compatible, bimanual, autoclavable, reusable etc., we propose a more general but distinct classification approach based on the actuation unit architecture as presented in Fig. 7. The actuation kinematics of a CTR deals with the actuation block arrangement and the mechanism of deployment. There are two types of block arrangements — parallel and serial — and their combination can result in fully parallel, fully serial, or hybrid architectures (or actuation units). For fully parallel architectures, the translations and rotations of each block are decoupled, as each one is independent and specific to one particular tube. For fully serial types, the translation or rotation in each block is mechanically coupled to the preceding actuation blocks, thereby influencing the resultant movement of the preceding tubes with respect to the actuation unit base. For hybrid architectures, the translations are coupled, but the rotations remain independent. The actuation unit prototypes presented to date in the literature fall into either the parallel or the hybrid category, with no examples of prototypes based on the serial architecture. In this section, we discuss the general components of all actuation units, followed by key aspects of each distinct actuation unit architecture.

A. Actuation Unit Elements

Irrespective of the choice of the actuation unit architecture or design requirements, the actuation unit of a CTR is always located at the proximal end of the tubes and contains the following essential elements.

- 1) Translation Stage: this section of the actuation block controls the translation of the tube, and its design determines the overall range of motion for the associated tube. Common components include: a rail-guide, a gear/belt/screw drive, an actuator (brushed DC motor, stepper motor, brushless DC motor, pneumatic or piezoelectric drive), and position sensor.
- 2) Rotation Stage: this section of the actuation block houses the mechanism/components for the rotational motion about the tube axis. The components that are associated with this section include gears, pulleys, bearings, actuators, and sensors.
- 3) Tube Holders: these elements are used to grasp the CTR tubes during deployment. While they can deform and potentially block inner tubes, screws radially pressing on the tubes have been used. Custom chucks as well as compressed rubber rings have also been used [144] and enable detachable designs, which can make sterilization easier. Glue has been used as well but results in permanent attachment.
- 4) Support Frame: this part serves as the main platform, upon which the other parts of the actuation unit are attached, and provides the necessary support during actuation.

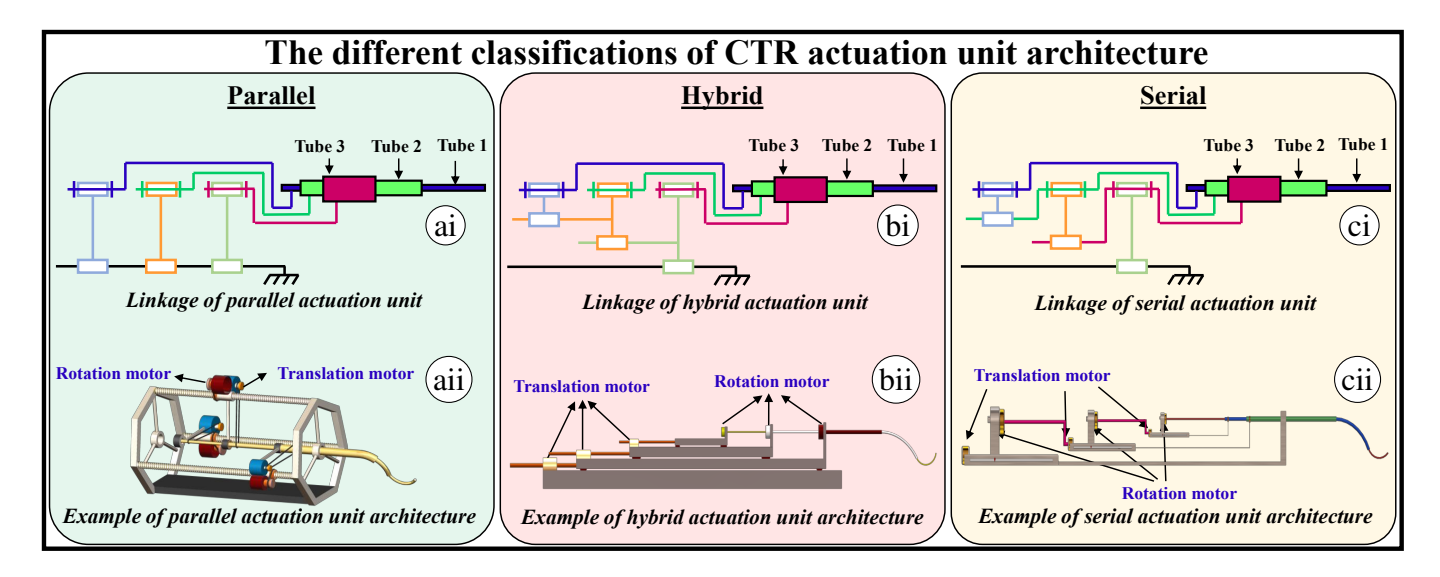


Fig. 7. The different classifications of CTR actuation units ai) The kinematic graph of parallel actuation unit, aii) The structural example of parallel actuation unit, bi) The kinematic graph of hybrid actuation unit, bii) The structural example of hybrid actuation unit, cii) The kinematic graphs of serial actuation unit, cii) The structural example of serial actuation unit.

B. Parallel Actuation Units

This category of actuation units operates based on a parallel actuation architecture, as shown in Fig. 7ai and 7aii for the kinematic graph and the structural design, respectively. Although their structural design, which depends on the type of actuation components and coupling mechanism used, might differ in construction or appearance, as shown in Fig. 8, their kinematics remain the same. The parallel architecture is the most commonly used actuation unit in the literature, as can be seen in our online CTR Prototyping Resources

One example of a parallel actuation unit was presented by Swaney et al. in [145], where the actuation unit also incorporates a puncturing mechanism (Fig. 8a). Another example of a system with a parallel architecture was presented by Hendrick et al. in [146], and illustrated in Fig. 8b. This system was designed to actuate two CTRs and has the benefit of being hand-held, with passive attachments to compensate for the weight of the device. Another parallel actuation unit prototype presented by Gosline et al. in [76], has a protruded front design that helps to reduce the interference caused by having the bulk actuation unit close to the patient and thereby, provides more free space in case other medical devices are to be introduced as well (Fig. 8c). Esakkiappan et al. proposed a 50 cm long CTR prototype composed of two tubes with 3 DOF in total and actuated via a parallel actuation unit [148]. The actuation unit uses stepper motors with rotary pulley mechanisms (Fig. 8e). Morimoto et al. in [11], [150], presented a compact, lightweight, hand-held and parallel actuation unit, where all the mechanical parts except the motors were fabricated using additive manufacturing. The design uses roller gears to enable rotation and translation in a compact form factor, along with a decoupled actuating structure, where each tube is controlled by an independent detachable actuation block (Fig. 8f). Another parallel CTR actuation unit prototype was presented by Xu in [149]. It was designed for teleoperated surgical tasks (Fig. 8g). The 6 DOF CTR can be controlled by

a haptic device. Finally, Swaney et al. designed a multi-arm 24 DOF CTR for single-nostril skull base surgery [147]. This parallel CTR actuation unit contains four independent sub-actuation units for simultaneous deployment of 4 arms, each of them being composed of 3 tubes, all actuated in rotation and translation (Fig. 8d).

The popularity of parallel actuation units can be explained by several factors. First, compared to hybrid or serial systems, it is easier to make parallel actuation units with modular components and actuation blocks. Indeed, the independence between each block enables the removal of some of the integration constraints that are inherent to serial and hybrid actuation units due to mechanical couplings between the blocks. Such modularity could have also lead to more cost-effective designs. In addition, the positioning accuracy in translation and rotation relative to the actuation unit base is better in parallel actuation units, since there is no error accumulation due to stacking of the actuation blocks.

C. Hybrid Actuation Units

The hybrid actuation architecture combines the serial and parallel block arrangements, resulting in interconnected blocks. Fig. 7bi and Fig. 7bii show a case study of hybrid kinematics and structural design, respectively, with translation blocks placed in series and rotation blocks placed in parallel. This structure is common in the literature for hybrid architectures, as shown in Fig. 9.

Several hybrid actuation units have been developed to date. For example, an MRI compatible, hybrid actuation unit was proposed by Su et al. in [151]. They created a 6 DOF, piezo-electrically actuated prototype to enable MRI-guided deployment of a precurved and steerable CTR. As shown in Fig. 9a, this design consists of different translation stages assembled on top of each other, which results in a simultaneous movement of all modules placed on top of the actuated one, while each tube rotates independently. Another hybrid, but manually

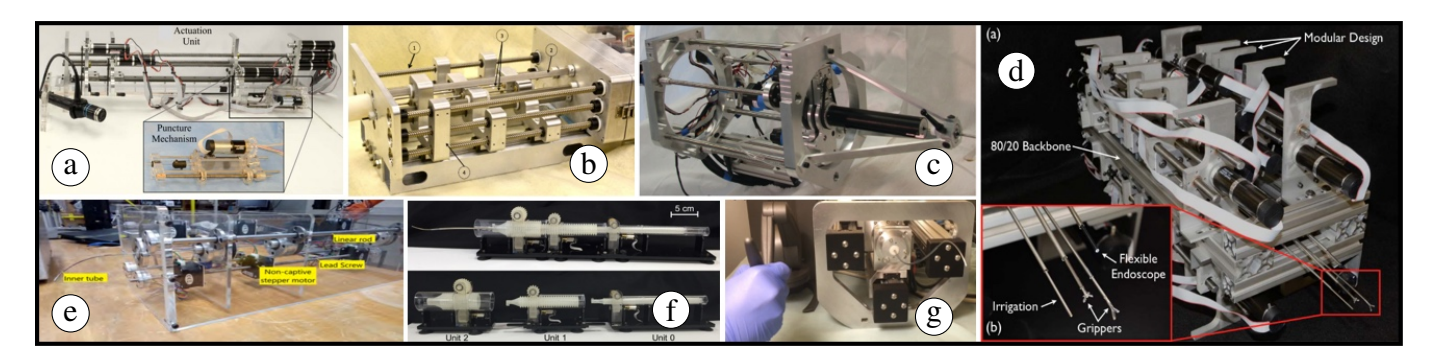


Fig. 8. Different parallel actuation unit prototypes a) An actuation unit with a puncturing mechanism by Swaney et al [145] ©[2015] IEEE, b) A multi-arm CTR actuation unit composing of 1) Lead screws connect translational motors in the motor pack to each carrier. 2) Square shafts connect rotational motors to tube bases through gear trains. 3) Tubes of the concentric tube manipulators can be seen here. 4) Tube carrier, by Hendrick et al [146] ©[2014] IEEE, c) A parallel actuation unit with a nose-like design structure by Gosline et al. in [76], d) A 4-arm 24 DOF CTR parallel actuation unit with 3 fully-actuated tubes per arm by Swaney et al. in [147], e) A transparent casing 3 DOF actuated unit by Esakkiappan et al. in [148] ©[2019] IEEE, f) A novel parallel actuation unit with a roller gear mechanism fabricated using additive manufacturing by Morimoto et al. in [11] ©[2017] IEEE, and g) A teleoperated CTR with parallel actuation unit by Xu in [149].

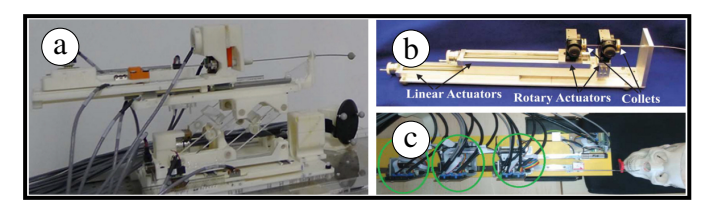


Fig. 9. The hybrid actuation unit prototypes, with a) MRI compatible 6-DOF piezoelectric actuation unit by Su et al. in [151], b) Manually actuated unit with precise tube positioning by Rucker et al. in [152] ©[2010] IEEE, c) Structurally linked hybrid actuation unit by Boushaki in [5], [153] ©[2016] IEEE.

actuated design, was developed by Rucker et al. in [152]. As shown in Fig. 9b, it was used to actuate two tubes with the outer tube held at a fixed location, while the inner tube was translated to five different positions and rotated to eight evenly spaced angular positions for each translation step. Finally, Boushaki et al. in [5], presented a hybrid actuation unit with all three translations arranged in series and rotations arranged in parallel, as shown in Fig. 9c.

Compared to some parallel actuation unit prototypes that have their translation stages attached at fixed locations with limited stroke, a benefit of the hybrid architecture is the increased stroke length achieved via the translation of the translation stages relative to the actuation unit base. However, this benefit comes at the cost of a lower absolute positioning accuracy in translation relative the actuation unit base, since the translation stages are stacked in series.

D. Serial Actuation Units

Noteworthy to mention is the serial actuation architecture, which is characterized by a purely serial arrangement, as shown in Fig. 7ci and 7cii, for the kinematics and structural design respectively. Here, each individual actuation is mechanically coupled to one another, thereby resulting in simultaneous transmission of actuation to all the preceding blocks. The idea of this particular actuation unit architecture has already been presented in the literature (see [4], [5]), but to date, there have not been any prototypes with this type of ar-

chitecture, as visible in our online CTR Prototyping Resources https://cgirerd.github.io/ctr_prototyping_resources.html.

The lack of developed prototypes could be explained by several reasons. First, the actuated degrees of freedom of such serial architectures are coupled. This feature is only useful in special cases, such as FTL deployment, where tubes need to follow a sequential deployment sequence that requires groups of tubes to move at the same velocity [46], [47]. However, because tubes must move at different velocities for general CTR deployment, the serial actuation architecture does not typically simplify the actuation strategy. Second, since the actuation stages of serial architectures are stacked on each other, the absolute position accuracy of the tubes relative to the base of the actuation unit is lower in translation and rotation compared to parallel architectures, and lower in rotation compared to the hybrid architectures proposed to date, since positioning errors add up. Third, stacking the actuation stages on top of each other also results in the center of mass of the actuation unit moving more than for parallel or hybrid architectures, since the bases of the motor supports are also required to move. To conclude, the serial architecture seems to have some downsides, but could potentially be used advantageously for CTR with FTL deployment, where their architecture is well-suited to the required actuation sequence.

E. Actuation Units: Perspectives

CTR development has mainly been focused on the tubes, while actuation units were simply viewed as means for moving them. However, with the maturation of the field, researchers have come to realize the importance of actuation units for general CTR performance. In addition, design features, such as sterilizability, required for commercial use, are becoming of interest and will place more focus on the actuation unit design. In fact, when designing a CTR actuation unit, there are several critical parameters that must be considered. First, the application itself dictates several constraints on the robot deployment and workflow. These constraints will inform, for example, whether the design must be MRI compatible, sufficiently compact or even hand-held, and which portions must

be sterilizable. The application will also affect the number of tubes required and the types of actuation sequences needed. Second, one must select an actuation unit architecture that is most suitable based on the given design constraints. This selection will involve weighing the relative benefits and complexities of the architectures. To date, the parallel architecture has been the most widely used, thanks to its simplicity, modular design, and high accuracy. Hybrid architectures with translation actuators in series have also been proposed, and can expand the translation stroke of some parallel architecture designs. While the serial architecture could be of interest for FTL deployment, its downsides have limited its development so far. Third, one must determine the structural design and elementary components for the actuation unit. Irrespective of having the same actuation unit architecture, the structural design and components differ based on application and available material, as shown in Fig. 8. Finally, the actuation unit must be physically built, assembled, and calibrated. Appropriate design and fabrication techniques must be selected for its structure, while other components such as motors, gears, nuts and screw rods, must typically be purchased.

There are numerous additional challenges associated with CTR actuation unit design. In particular, there are several requirements that must be met to ensure compatibility in a clinical setting, including sterilizability, safety, compatibility with associated medical imaging, and ease of integration in the clinical workflow. While several of these requirements were often overlooked in much of the older literature, researchers have recently started to design actuation systems with the goal of meeting these needs. For example, Graves et al. [154] proposed a compact and inexpensive CTR design, which has the potential for one-time use and is disposable after surgery. Burgner et al. in [155] proposed a manually actuated, reusable approach, consisting of an actuation unit that is autoclavable and requires no oil lubrication. Burgner et al. in [68], then extended the reusable approach by creating a sterilizable and biocompatible design that uses a sterile bag/drape to isolate the detachable motor pack from the other autoclave sterilized parts of the robot, and this concept has since been adopted for multiple designs [24], [44], [140]. In order to address the issue of MRI compatibility and integration with existing clinical workflows, researchers have proposed the use of either pneumatic or piezoelectric actuators. However, there are only a handful of such designs in the literature (refer to our online CTR Prototyping Resources https://cgirerd.github.io/ctr prototyping resources.html), likely due to their control complexity and size. Since CTRs are mostly used for medical interventions, sterilization considerations become very important. Yet this aspect is not significantly discussed in the literature, with little detail on the use/design of a sterile boundary or isolation drape. Finally, our proposed classification system based on the actuation unit architecture in Fig. 7, could be used to uniquely identify and categorize new CTR prototypes (as used https://cgirerd.github.io/ctr_prototyping_resources.html),

and to ease the selection/development of an architecture.

V. END EFFECTORS

The last component of a CTR is the end effector, which is deployed at the tip. There are many innovative designs, and they can be classified based on the task to be performed. We focus here on designs for manipulation, inspection, excision and resection, and navigation.

A. Manipulation

Many end effectors are designed for manipulating objects or tissues at the surgical site. The types of manipulations to be performed include grasping, retracting, stabilizing, holding, gripping, turning, tilting, picking, placing, adjusting, pushing or pulling. Burgner et al. in [156], proposed a prototype with two different end effectors, shown in Fig. 10a. The first consists in a 4 mm long gripper with 110° of opening angle when fully opened, that was disassembled from a flexible grasper (Endo-Jaw, FB-211K, Olympus, Japan) and assembled at the tip of the innermost tube of a CTR. The second is an ellipse-like steel ribbon curette (with a major radius of 2 mm, a minor radius of 1.75 mm and a height 1.15 mm), which was attached directly to the innermost tube. Dupont et al. in [7] presented a 1 mm diameter tip mounted forceps, shown in Fig. 10b, which is connected to a wire deployed inside the CTR and linearly actuated to open or close the forceps tip. A multi-arm CTR proposed by Wang et al. in [157] consists of a remotely-controlled 1.8 mm diameter medical forceps end effector connected to a 6 DOF CTR for manipulation purposes, as shown in Fig. 10c. Lin et al. in [93], presented a gripper design consisting of a 300 μ m diameter steel forceps, which are welded to a 27G stainless steel tubing and glued to the CTR distal tip as shown in Fig. 10d. The forceps is used for gripping by pushing-out or pulling-in of the attached Nitinol wire, in order to open or close the gripper respectively. Yu et al. in [158], presented a multi-arm CTR prototype with two flexible, sterilized end effectors which are deployed through the inner tube. One of these end effectors consisted of a 1.8 mm diameter mini forceps pair for tissue grasping, as shown in Fig. 10e. Dupont et al. in [163], demonstrated a CTR with a gripper for tissue manipulation during laser dissection operation.

B. Inspection

This category of end effectors includes the use of lighting sources and cameras (e.g. for endoscopic usage) for in vivo visualization of the area of interest during navigation or at the surgical site. One example is the three arm CTR system proposed by Wang et al. in [157], in which one of the CTR outlet channels contains a 4 DOF active vision arm. This arm is attached to an endoscope, which is used for visual feedback as shown in Fig. 10c. Another example was presented by Yu et al. [158], where a multi-arm CTR prototype was equipped with a 4 mm diameter vision channel, having a 110° lens view angle endoscope attached at the tip for visual feedback (Fig. 10e). Girerd et al. [162], demonstrated the use of an RGB camera at the tip of a CTR, for visualising and detecting areas during a simultaneous localization and mapping deployment

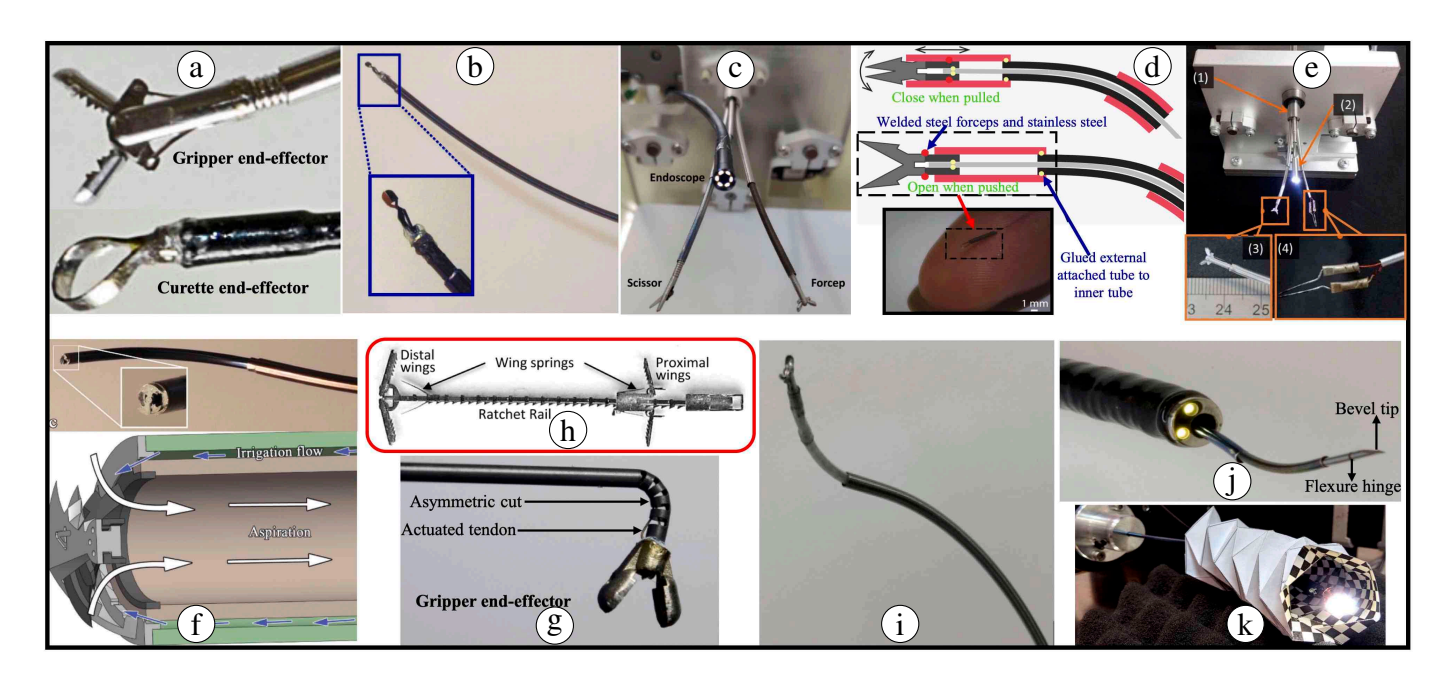


Fig. 10. Different CTR end effector prototypes: a) Gripper and curette end effectors [156] ©[2014] IEEE b) Tip mounted forceps end effector [7] ©[2009] IEEE, c) Multi-arm CTR with scissors and forceps [157], d) The design description and prototype of forceps gripper end effector [93] ©[2015] IEEE, e) A multi-channel CTR with forceps pair for tissue grasping and electric coagulator for tissue ablation [158] ©[2016] IEEE, f) Tissue removing end effector design prototype [159], h) Metal MEMS tissue approximation detachable end effector [76], g) Needle-sized wrist gripper [160], i) Cable driven CTR disposable micro end effector [161] ©[2016] IEEE, j) Beveled tip end effector [145] ©[2015] IEEE, k) RGB camera end effector navigating through an origami tunnel [162] ©[2020] IEEE.

strategy with approximate FTL behavior, through an origami tunnel (Fig. 10k).

C. Excision/Resection

This category of end effectors includes mechanisms that enable cutting, puncturing, stitching, excision, ablation or dissection. These tasks are common across many procedures and a number of different prototypes have been developed for such purposes. For example, Wang et al. in [157], proposed a multi-arm CTR with one arm equipped with a remotely controlled 2 mm diameter scissor end effector (Fig. 10c) for dissection inside the skull. Vasilyev et al. [159] proposed a surgical device with tissue removal capabilities for a beating heart surgery. The prototype is fabricated using a special metal manufacturing MEMS process (eFAB by Microfabrica), which enables the incorporation of micron-scale features into a single device that is deployed through a steerable CTR to the surgical site. The prototype incorporates both aspiration and irrigation features for tissue removal and is shown in Fig. 10f. Yu et al. in [158] presented a multi-arm CTR prototype with two end effectors, including a customized electric coagulator for tissue ablation, as shown in Fig. 10e. In addition, Gosline et al. proposed a detachable end effector, shown in Fig. 10h, which was prototyped using metal additive manufacturing [76]. It was designed to close or seal abnormal openings, such as the heart atria, by puncturing, pulling, and stitching two tissue layers together. Another aspect is the suction operation, which was achieved by connecting an aspirator at the end of the innermost cannula, for intracerebral hemorrhage evacuation as presented in [68], [164]. Finally, there are areas where CTRs are used

for tissue cutting, by passing fibre optics with a laser through the innermost tube to the surgical site, as demonstrated in the same video by Dupont et al. in [163]. This technique of using fibre optics was further extended to laser ablation of real cholesteatoma cells in [127] and also, for laser-induced thermotherapy in the brain [165].

D. Hybridized Architectures

In order to improve the dexterity at the distal end of the CTR end effector and achieve stringent pose requirements in confined spaces, hybridized robot architectures have been proposed. These mechanisms involve the integration of another form of actuation, such as tendons or flexure hinges, at the distal end. Prasai et al. in [161] demonstrated a 2 mm diameter, cable-driven end effector using a polyolefin tube and acrylic and steel strings. It can be mounted on a CTR as shown in Fig. 10i and has the ability to bend in all directions using the three control cables spaced 120° apart. Another example is a needle-sized wrist design that can be used to maneuver around tight corners [160]. This end effector, which was presented by Swaney et al., is tendon actuated and composed of an asymmetrically patterned nitinol tube designed to reach tighter curvatures with lower tendon actuation forces. It also contains an attachable ring curette or gripper, as shown in Fig. 10g. One drawback of the asymmetric cutouts is that it is limited to one directional bending, compared to the design of Prasai et al. in [161], which can bend in all directions. Other asymmetrically cut nitinol tube designs were investigated by Eastwood et al. in [166]. Swaney et al. in [145], presented a functionalized needle with a spring-loaded puncturing mechanism for tissue

opening. The steerable needle consists of a flexure joint, as shown in Fig. 10j, and helps to follow higher curvature paths through tissue.

E. End Effectors: Perspectives

The end effectors have traditionally been the least discussed topic in the CTR literature, due to the focus on tube geometries first, then followed by the actuation units. Typically, the size of a CTR decrease from the proximal to the distal end (i.e. from the actuation unit to the tubes themselves and finally to the end effector). Moreover, the end effector has to be deployed or integrated at the tip of the smallest (innermost) tube of the robot, which means that the end effector must be small (millimeter scale or less). Due to the desire to further decrease surgical invasiveness and to enable multi-arm deployment via a single port, further miniaturization of the tube dimensions will likely be needed. These requirements pose a great challenge for the realization of submillimeterscale end effectors. Difficulties in fabricating, integrating and actuating such small-scale end effectors likely explains why there are very few end effectors reported in the literature to date. In fact, researchers often use end effectors taken directly from off-the-shelf medical tools, rather than designing their own. These remaining challenges call for significant dedicated research with regards to the design and fabrication of customized/miniaturized end effectors, capable of fitting and taking advantage of the small hollow passage of the internal tube. Concerning the drawbacks on the micro fabrication of end effectors, the focus on developing systems for commercial use, could potentially boost its development in the future. One notable missing aspect in the literature is the implementation of interchangeable end-effector designs. This capability would enable robots to easily perform multiple functions without the need to change the entire tube set or actuation system.

VI. CONCLUSION AND DISCUSSION

This survey paper aims to provide a single resource with the details of all CTR prototypes. The focus is on the various CTR designs and fabrication methods for the main three components of a CTR represented in Fig. 1: the tubes, the actuation unit, and the end effector. In addition to identifying the different approaches and technologies for the various CTR designs presented in the literature, we also proposed a new way of classifying CTRs based on their actuation architecture (serial, parallel, or hybrid). We believe that this review can serve as a basis for the benchmarking of CTR prototypes and can help researchers better design their robots. In addition, we highlighted the main future opportunities for CTRs with respect to the tube design, tube fabrication, actuation unit, and end effector.

Furthermore, as previously discussed, it is important to think about a path towards commercialization. Despite the significant research advances over the years and the numerous prototypes developed for different applications, there is still no single commercially available product [167]. One of the major deterrents could be the long time to market certification for medical robotic systems. We note that Virtuoso Surgical is

the furthest along this path towards commercialization and has currently advanced to clinical trials in the operating room [32], [168]. Yet the majority of research groups still seem focused on addressing the remaining scientific challenges, which often ends in a CTR prototype, rather than on advancing towards commercialization. Grassmann et al. in [167], have noted a current practice in the research community of rarely reusing CTR prototypes across individual research groups. This low reuse rate is likely due to the fact that robot-base evaluations do boost the chances of paper acceptance, and this trend has hindered fast advancement and development of a single, widely-used robotic platform. Given all of the above, it is important as a community to start finding paths towards commercialization, potentially through the development of a mature robotics platform, as suggested by Grassmann et al. [167]. As such, it would be beneficial for the research community to establish an open-source repository where members can share details of their robot prototype, including the mechatronics design, CAD, and hardware schematics for rapid advancement and contribution to the field of knowledge.

Finally, it is important to look at concentric tube robots in the broader context of the continuum robotics field. Indeed there are several other classes of continuum robots, notably tendon-driven and multi-backbone robots, that similarly offer potential improvements to existing medical procedures due to their inherent compliance and ability to navigate around highly curved paths. These potential benefits have motivated the development of numerous continuum robotic platforms, and in turn, a large increase in the number of publications in this area over the last decade [169]. It should also be noted that with the rise in popularity of soft robotics, there has also been an increase in the development of soft continuum robots, made from compliant materials [169]. While such robots can offer even more added safety, they may have difficulty in applying sufficient forces for many surgical interventions and tissue manipulation tasks [170]. And as these fields of soft robotics, soft continuum robotics, and continuum robotics continue to advance, quantitative assessment of the benefits and tradeoffs among various robotic platforms will become critical for truly enabling the successful transition of prototypes from the bench-top to the clinic.

REFERENCES

- R. J. Webster III, "Design and Mechanics of Continuum Robots for Surgery," Doctoral dissertation, Johns Hopkins University, 2007.
- [2] J. Burgner, P. J. Swaney, D. C. Rucker, H. B. Gilbert, S. T. Nill, P. T. Russell, K. D. Weaver, and R. J. Webster III, "A bimanual teleoperated system for endonasal skull base surgery," in *IEEE/RSJ International Conference on Intelligent Robots and Systems*, 2011, pp. 2517–2523.
- [3] H. Gilbert, R. Hendrick, A. Remirez, and R. Webster, "A robot for transnasal surgery featuring needle-sized tentacle-like arms," in Expert Review of Medical Devices, vol. 11, no. 1, pp. 5–7, 2014.
- [4] H. Alfalahi, F. Renda, and C. Stefanini, "Concentric tube robots for minimally invasive surgery: Current applications and future opportunities," *IEEE Transactions on Medical Robotics and Bionics*, vol. 2, no. 3, pp. 410–424, 2020.
- [5] M. N. Boushaki, "Design Optimization and Control for Concentric Tube Robot in Assisted Single-Access Laparoscopic Surgery," Doctoral dissertation, Université Montpellier, Oct. 2016.

- [6] J. Burgner-Kahrs, D. C. Rucker, and H. Choset, "Continuum Robots for Medical Applications: A Survey," in *IEEE Transactions on Robotics*, vol. 31, no. 6, pp. 1261–1280, 2015.
- [7] P. E. Dupont, J. Lock, and E. Butler, "Torsional kinematic model for concentric tube robots," in *IEEE International Conference on Robotics* and Automation, 2009, pp. 3851–3858.
- [8] P. E. Dupont, J. Lock, B. Itkowitz, and E. Butler, "Design and control of concentric-tube robots," in *IEEE Transactions on Robotics*, vol. 26, no. 2, pp. 209–225, 2010.
- [9] P. E. Dupont, J. Lock, and B. Itkowitz, "Real-time position control of concentric tube robots," in *IEEE International Conference on Robotics* and Automation, 2010, pp. 562–568.
- [10] C. Bergeles, A. H. Gosline, N. V. Vasilyev, P. J. Codd, P. J. del Nido, and P. E. Dupont, "Concentric tube robot design and optimization based on task and anatomical constraints," in *IEEE Transactions on Robotics*, vol. 31, no. 1, pp. 67–84, 2015.
- [11] T. K. Morimoto, E. W. Hawkes, and A. M. Okamura, "Design of a compact actuation and control system for flexible medical robots," in IEEE Robotics and Automation Letters, vol. 2, no. 3, pp. 1579–1585, 2017.
- [12] R. J. Webster, A. M. Okamura, and N. J. Cowan, "Toward active cannulas: Miniature snake-like surgical robots," in *IEEE/RSJ International Conference on Intelligent Robots and Systems*, 2006, pp. 2857–2863.
- [13] P. Sears and P. Dupont, "A steerable needle technology using curved concentric tubes," in *IEEE/RSJ International Conference on Intelligent Robots and Systems*, 2006, pp. 2850–2856.
- [14] H. B. Gilbert, D. C. Rucker, and R. J. Webster III, Concentric Tube Robots: The State of the Art and Future Directions. Robotics Research. Springer Tracts in Advanced Robotics, 2016, pp. 253–269.
- [15] R. J. Webster, J. M. Romano, and N. J. Cowan, "Mechanics of precurved-tube continuum robots," *IEEE Transactions on Robotics*, vol. 25, no. 1, pp. 67–78, 2009.
- [16] A. Mahoney, H. Gilbert, and R. Webster, A Review of Concentric Tube Robots: Modeling, Control, Design, Planning, and Sensing. Encyclopedia of Medical Robotics, Minimally Invasive Surgical Robotics, 2016, pp. 181–202.
- [17] R. J. Webster and B. A. Jones, "Design and kinematic modeling of constant curvature continuum robots: A review," *International Journal* of Robotics Research, vol. 29, no. 13, pp. 1661–1683, 2010.
- [18] I. D. Walker, "Continuous Backbone "Continuum" Robot Manipulators," ISRN Robotics, pp. 1–19, 2013.
- [19] W. Robert, James, A. M. Okamura, N. J. Cowan, and R. H. Taylor, "Active cannula for bio-sensing and surgical intervention," U.S. Patent US008 715 226B2, May 06, 2014.
- [20] T. Karen I, "Active cannula configuration for minimially invasive surgery," U.S. Patent US009 895 163B2, Feb. 20, 2018.
- [21] C. Seneci, C. Bergeles, and L. Da cruz, "Actuation system for tubes of a robotic tool," United Kingdom Patent WO2 021 148 797A1, Jul. 29, 2021.
- [22] A. Zenati, Marco and M. Mohammady, Mahsen, "Hybrid snake robot for minimally invasive intervention," United State Patent WO2 013 026 012A1, Feb. 21, 2013.
- [23] R. Hendrick, N. Dillon, E. Blum, and L. Branscombe, "Concentric tube apparatus for minimally invasive surgery," U.S. Patent US20 220 241 029A1, Aug. 04, 2022.
- [24] R. J. Hendrick, I. Robert J. Webster, S. D. Herrell, P. J. Swaney, and R. Lathrop, "Concentric tube robot," U.S. Patent US010441371B2, Oct. 15, 2019.
- [25] P. Dupont and K. Price, "Bimanual neuroendoscopic robot," U.S. Patent US20 210 228 296A1, Jul. 29, 2021.
- [26] P. J. Swaney, R. Lathrop, J. Burgner, K. Weaver, H. B. Gilbert, R. J. Webster, and D. B. Comber, "System ,method , and apparatus for configuration , design , and operation of an active cannula robot," U.S. Patent US010 548 630B2, Feb. 04, 2020.
- [27] J. Neimat, E. Barth, R. Webster, and D. Comber, "System and apparatus for performing transforminal therapy," U.S. Patent WO2 015 073 943A1, May 21, 2015.
- [28] S. D. Herrell, R. J. Webster, T. Bruns, P. J. Swaney, and R. Hendrick, "System and method for endoscopic deployment of robotic concentric tube manipulators for performing surgery," U.S. Patent US010 238 457B2, Mar. 26, 2019.
- [29] L. Yu, Alan, "Robotically controlled steerable catheters," U.S. Patent US20140364870A1, Mar. 22, 2012.
- [30] R. Alterovitz, L. G. Torres, P. J. Swaney, H. B. Gilbert, R. J. Webster, and R. J. Hendrick, "Methods, systems, and computer readable media for controlling a concentric tube probe," U.S. Patent US010 846 928B2, Nov. 24, 2020.

- [31] R. Lathrop, T. L. Bruns, A. W. Mahoney, H. B. Gilbert, P. J. Swaney, R. J. Hendrick, K. Weaver, P. T. Russell, S. D. Herrell, and R. J. Webster, "Modular sterilizable robotic system for endonasal surgery," U.S. Patent US010 307 214B2, Jun. 04, 2019.
- [32] Z. Mitros, S. Sadati, R. Henry, L. Cruz, and C. Bergeles, "From theoretical work to clinical translation: Progress in concentric tube robots," *Annual Review of Control Robotics and Autonomous Systems*, vol. 5, 01 2021.
- [33] R. Grassmann, V. Modes, and J. Burgner-Kahrs, "Learning the forward and inverse kinematics of a 6-dof concentric tube continuum robot in se(3)," in 2018 IEEE/RSJ International Conference on Intelligent Robots and Systems (IROS), 2018, pp. 5125–5132.
- [34] A. Vandini, C. Bergeles, F.-Y. Lin, and G.-Z. Yang, "Vision-based intraoperative shape sensing of concentric tube robots," in 2015 IEEE/RSJ International Conference on Intelligent Robots and Systems (IROS), 2015, pp. 2603–2610.
- [35] A. V. Kudryavtsev, M. T. Chikhaoui, A. Liadov, P. Rougeot, F. Spindler, K. Rabenorosoa, J. Burgner-Kahrs, B. Tamadazte, and N. Andreff, "Eye-in-Hand Visual Servoing of Concentric Tube Robots," *IEEE Robotics and Automation Letters*, vol. 3, no. 3, pp. 2315–2321, 2018.
- [36] R. Xu, A. Yurkewich, and R. V. Patel, "Shape sensing for torsionally compliant concentric-tube robots," in *Optical Fibers and Sensors for Medical Diagnostics and Treatment Applications XVI*, I. Gannot, Ed., vol. 9702, International Society for Optics and Photonics. SPIE, 2016, p. 97020V. [Online]. Available: https://doi.org/10.1117/12.2213128
- [37] S. C. Ryu and P. E. Dupont, "Fbg-based shape sensing tubes for continuum robots," in 2014 IEEE International Conference on Robotics and Automation (ICRA), 2014, pp. 3531–3537.
- [38] V. Modes and J. Burgner-Kahrs, "Calibration of concentric tube continuum robots: Automatic alignment of precurved elastic tubes," *IEEE Robotics and Automation Letters*, vol. 5, no. 1, pp. 103–110, 2020.
- [39] S. Song, Z. Li, H. Yu, and H. Ren, "Electromagnetic positioning for tip tracking and shape sensing of flexible robots," *IEEE Sensors Journal*, vol. 15, no. 8, pp. 4565–4575, 2015.
- [40] V. Arabagi, A. Gosline, R. J. Wood, and P. E. Dupont, "Simultaneous soft sensing of tissue contact angle and force for millimeter-scale medical robots," in 2013 IEEE International Conference on Robotics and Automation, 2013, pp. 4396–4402.
- [41] B. Xu and S. Y. Ko, "Novel force sensing module for a concentric tube-based vitreoretinal surgical robot," Sensors and Actuators A: Physical, vol. 316, p. 112395, 2020. [Online]. Available: https://www.sciencedirect.com/science/article/pii/S0924424720317118
- [42] J. Furusho, T. Ono, R. Murai, T. Fujimoto, Y. Chiba, and H. Horio, "Development of a curved multi-tube (cmt) catheter for percutaneous umbilical blood sampling and control methods of cmt catheters for solid organs," in *IEEE International Conference Mechatronics and Automation*, 2005, vol. 1, 2005, pp. 410–415 Vol. 1.
- [43] T. Anor, J. Madsen, and P. Dupont, "Algorithms for design of continuum robots using the concentric tubes approach: A neurosurgical example," in IEEE International Conference on Robotics and Automation, ICRA, pp. 667–673, 05 2011.
- [44] R. J. Hendrick, C. R. Mitchell, S. D. Herrell, and R. J. Webster, "Hand-held transendoscopic robotic manipulators: A transurethral laser prostate surgery case study," *International Journal of Robotics Re*search, vol. 34, no. 13, pp. 1559–1572, 2015.
- [45] H. B. Gilbert and R. J. Webster, "Can concentric tube robots follow the leader?" in *IEEE International Conference on Robotics and Au*tomation, 2013, pp. 4881–4887.
- [46] H. B. Gilbert, J. Neimat, and R. J. Webster, "Concentric tube robots as steerable needles: Achieving follow-the-leader deployment," *IEEE Transactions on Robotics*, vol. 31, no. 2, pp. 246–258, 2015.
- [47] A. Garriga-Casanovas and F. Rodriguez y Baena, "Complete follow-the-leader kinematics using concentric tube robots," *International Journal of Robotics Research*, vol. 37, no. 1, pp. 197–222, 2018.
- [48] R. J. Webster, J. M. Romano, and N. J. Cowan, "Kinematics and calibration of active cannulas," in *IEEE International Conference on Robotics and Automation*, 2008, pp. 3888–3895.
- [49] D. C. Rucker and R. J. Webster, "Parsimonious evaluation of concentric-tube continuum robot equilibrium conformation," *IEEE Transactions on Biomedical Engineering*, vol. 56, no. 9, pp. 2308–2311, 2009.
- [50] D. C. Rucker, R. J. Webster III, G. S. Chirikjian, and N. J. Cowan, "Equilibrium conformations of concentric-tube continuum robots," *The International Journal of Robotics Research*, vol. 29, no. 10, pp. 1263–1280, 2010.

- [51] J. Lock and P. E. Dupont, "Friction modeling in concentric tube robots," IEEE International Conference on Robotics and Automation, pp. 1139– 1146, 2011.
- [52] J. Ha, G. Fagogenis, and P. E. Dupont, "Modeling tube clearance and bounding the effect of friction in concentric tube robot kinematics," *IEEE Transactions on Robotics*, vol. 35, no. 2, pp. 353–370, 2019.
- [53] D. C. Rucker, B. A. Jones, and R. J. Webster, "A model for concentric tube continuum robots under applied wrenches," in 2010 IEEE International Conference on Robotics and Automation, 2010, pp. 1047–1052.
- [54] J. Granna, "Multi-objective particle swarm optimization for the structural design of concentric tube continuum robots for medical applications," *Doctoral dissertation, Hannover: Gottfried Wilhelm Leibniz Universität*, 2019.
- [55] J.-T. Lin, C. Girerd, J. Yan, J. Hwang, and T. K. Morimoto, "A generalized framework for concentric tube robot design using gradientbased optimization," *IEEE Transactions on Robotics (T-RO)*, 2022 (Accepted, to appear).
- [56] C. Baykal, C. Bowen, and R. Alterovitz, "Asymptotically optimal kinematic design of robots using motion planning," *Autonomous robots*, vol. 43, no. 2, pp. 345–357, 2019.
- [57] C. Baykal and R. Alterovitz, "Asymptotically optimal design of piecewise cylindrical robots using motion planning." in *Robotics: Science* and Systems, 2017.
- [58] C. Baykal, L. G. Torres, and R. Alterovitz, "Optimizing design parameters for sets of concentric tube robots using sampling-based motion planning," in *IEEE/RSJ International Conference on Intelligent Robots and Systems*, 2015, pp. 4381–4387.
- [59] L. G. Torres, R. J. Webster, and R. Alterovitz, "Task-oriented design of concentric tube robots using mechanics-based models," in *IEEE/RSJ International Conference on Intelligent Robots and Systems*, 2012, pp. 4449–4455.
- [60] C. Girerd, "Conception de robots à tubes concentriques et application à l'inspection des cellules olfactives," *Doctoral dissertation*, *Université* de Strasbourg, Jan. 2018.
- [61] M. Boushaki, C. Liu, B. Herman, V. Trevillot, M. Akkari, and P. Poignet, "Optimization of concentric-tube robot design for deep anterior brain tumor surgery," in 14th International Conference on Control, Automation, Robotics and Vision (ICARCV), 2016, pp. 1–6.
- [62] J. Ha, F. C. Park, and P. E. Dupont, "Optimizing Tube Precurvature to Enhance the Elastic Stability of Concentric Tube Robots," *IEEE Transactions on Robotics*, vol. 33, no. 1, pp. 22–37, 2017.
- [63] J. Ha, F. C. Park, and P. E. Dupont, "Achieving elastic stability of concentric tube robots through optimization of tube precurvature," in *IEEE/RSJ International Conference on Intelligent Robots and Systems*, 2014, pp. 864–870.
- [64] M. T. Chikhaoui, J. Granna, J. Starke, and J. Burgner-Kahrs, "Toward motion coordination control and design optimization for dual-arm concentric tube continuum robots," *IEEE Robotics and Automation Letters*, vol. 3, no. 3, pp. 1793–1800, 2018.
- [65] G. Noh, S. Y. Yoon, S. Yoon, K. Kim, W. Lee, S. Kang, and D. Lee, "Expeditious design optimization of a concentric tube robot with a heat-shrink plastic tube," in 2016 IEEE/RSJ International Conference on Intelligent Robots and Systems (IROS), 2016, pp. 3671–3676.
- [66] J. Granna, A. Nabavi, and J. Burgner-Kahrs, "Toward computer-assisted planning for interstitial laser ablation of malignant brain tumors using a tubular continuum robot," in *Medical Image Computing and Computer-Assisted Intervention (MICCAI 2017)*, M. Descoteaux, L. Maier-Hein, A. Franz, P. Jannin, D. L. Collins, and S. Duchesne, Eds. Cham: Springer International Publishing, 2017, pp. 557–565.
- [67] J. Granna, Y. Guo, K. D. Weaver, and J. Burgner-Kahrs, "Comparison of optimization algorithms for a tubular aspiration robot for maximum coverage in intracerebral hemorrhage evacuation," *Journal of Medical Robotics Research*, vol. 02, no. 01, p. 1750004, 2017.
- [68] J. Burgner, P. J. Swaney, R. A. Lathrop, K. D. Weaver, and R. J. Webster, "Debulking from within: A robotic steerable cannula for intracerebral hemorrhage evacuation," in *IEEE Transactions on Biomedical Engineering*, vol. 60, no. 9, pp. 2567–2575, 2013.
- [69] J. Burgner, H. B. Gilbert, and R. J. Webster, "On the computational design of concentric tube robots: Incorporating volume-based objectives," in *IEEE International Conference on Robotics and Automation*, 2013, pp. 1193–1198.
- [70] M. Farooq, B. Xu, and S. Y. Ko, "A concentric tube-based 4-DOF puncturing needle with a novel miniaturized actuation system for vitrectomy," *BioMedical Engineering OnLine*, vol. 18, 04 2019.
- [71] M. Farooq, S. Park, J. Park, and S. Ko, "Shape optimization of a novel ligation tool using a concentric tube mechanism," in 16th International Conference on Control, Automation and Systems, 2016, pp. 413–418.

- [72] T. K. Morimoto, J. D. Greer, E. W. Hawkes, M. H. Hsieh, and A. M. Okamura, "Toward the design of personalized continuum surgical robots," *Annals of Biomedical Engineering*, vol. 46, no. 10, pp. 1522–1533, 2018.
- [73] T. Morimoto, J. Cerrolaza, M. Hsieh, K. Cleary, A. Okamura, and M. G. Linguraru, "Design of patient-specific concentric tube robots using path planning from 3-d ultrasound," in *Annual International Conference of the IEEE Engineering in Medicine and Biology Society*, vol. 2017, 07 2017, pp. 165–168.
- [74] T. K. Morimoto, J. D. Greer, M. H. Hsieh, and A. M. Okamura, "Surgeon design interface for patient-specific concentric tube robots," in *IEEE/RAS-EMBS International Conference on Biomedical Robotics and Biomechatronics*, 2016, pp. 41–48.
- [75] C. Bedell, J. Lock, A. Gosline, and P. E. Dupont, "Design optimization of concentric tube robots based on task and anatomical constraints," in *IEEE International Conference on Robotics and Automation*, 2011, pp. 398–403.
- [76] A. H. Gosline, N. V. Vasilyev, E. J. Butler, C. Folk, A. Cohen, R. Chen, N. Lang, P. J. Del Nido, and P. E. Dupont, "Percutaneous intracardiac beating-heart surgery using metal mems tissue approximation tools," *International Journal of Robotics Research*, vol. 31, no. 9, pp. 1081– 1093, 2012.
- [77] P. Dupont, A. Gosline, N. Vasilyev, J. Lock, E. Butler, C. Folk, A. Cohen, R. Chen, G. Schmitz, and P. del Nido, "Concentric tube robots for minimally invasive surgery," *Hamlyn Symposium on Medical Robotics*, 01 2012.
- [78] C. Girerd, T. Lihoreau, K. Rabenorosoa, B. Tamadazte, M. Benassarou, L. Tavernier, L. Pazart, E. Haffen, N. Andreff, and P. Renaud, "In vivo inspection of the olfactory epithelium: Feasibility of robotized optical biopsy," *Annals of Biomedical Engineering (ABME)*, vol. 46, pp. 1951– 1961, Jun. 2018.
- [79] C. Baykal, "Design optimization algorithms for concentric tube robots," Master's thesis. University of North Carolina at Chapel Hill, 2015.
- [80] H. B. Gilbert and R. J. Webster, "Rapid, Reliable Shape Setting of Superelastic Nitinol for Prototyping Robots," *IEEE Robotics and Automation Letters*, vol. 1, no. 1, pp. 98–105, 2016.
- [81] J.-S. Kim, D.-Y. Lee, K. Kim, S. Kang, and K.-J. Cho, "Toward a solution to the snapping problem in a concentric-tube continuum robot: Grooved tubes with anisotropy," in *IEEE International Conference on Robotics and Automation (ICRA)*, 2014, pp. 5871–5876.
- [82] D. Y. Lee, J. Kim, J. S. Kim, C. Baek, G. Noh, D. N. Kim, K. Kim, S. Kang, and K. J. Cho, "Anisotropic Patterning to Reduce Instability of Concentric-Tube Robots," *IEEE Transactions on Robotics*, vol. 31, no. 6, pp. 1311–1323, 2015.
- [83] K. A. X. J. Luo, J. Kim, T. Looi, and J. Drake, "Design optimization for the stability of concentric tube robots," *IEEE Robotics and Automation Letters*, vol. 6, no. 4, pp. 8309–8316, 2021.
- [84] H. B. Gilbert, R. J. Hendrick, and R. J. Webster, "Elastic Stability of Concentric Tube Robots: A Stability Measure and Design Test," *IEEE Transactions on Robotics*, vol. 32, no. 1, pp. 20–35, 2016.
- [85] R. J. Hendrick, H. B. Gilbert, and R. J. Webster, "Designing snapfree concentric tube robots: A local bifurcation approach," in *IEEE International Conference on Robotics and Automation (ICRA)*, 2015, pp. 2256–2263.
- [86] Q. Peyron, K. Rabenorosoa, N. Andreff, and P. Renaud, "A numerical framework for the stability and cardinality analysis of concentric tube robots: Introduction and application to the follow-the-leader deployment," *Mechanism and Machine Theory*, vol. 132, pp. 176–192, 2019.
- [87] C. Girerd, K. Rabenorosoa, and P. Renaud, Combining Tube Design and Simple Kinematic Strategy for Follow-the-Leader Deployment of Concentric Tube Robots. Cham: Springer International Publishing, 2018, pp. 23–31.
- [88] C. Girerd, T. Schlinquer, N. Andreff, P. Renaud, and K. Rabenorosoa, "Design of concentric tube robots using tube patterning for follow-the-leader deployment," *Journal of Mechanisms and Robotics*, vol. 13, no. 1, pp. 1–10, Aug. 2020.
- [89] H. Azimian, P. Francis, T. Looi, and J. Drake, "Structurally-redesigned concentric-tube manipulators with improved stability," in *IEEE/RSJ International Conference on Intelligent Robots and Systems*, 2014, pp. 2030–2035.
- [90] K. A. Xin Jue Luo, T. Looi, S. Sabetian, and J. Drake, "Designing concentric tube manipulators for stability using topology optimization," in *IEEE/RSJ International Conference on Intelligent Robots and Systems (IROS)*, 2018, pp. 1764–1769.
- [91] M. Rox, M. Emerson, T. E. Ertop, I. Fried, M. Fu, J. Hoelscher, A. Kuntz, J. Granna, J. E. Mitchell, M. Lester, F. Maldonado, E. A.

- Gillaspie, J. A. Akulian, R. Alterovitz, and R. J. Webster, "Decoupling steerability from diameter: Helical dovetail laser patterning for steerable needles," *IEEE Access*, vol. 8, pp. 181411–181419, 2020.
- [92] C. Rucker, J. Childs, P. Molaei, and H. B. Gilbert, "Transverse anisotropy stabilizes concentric tube robots," *IEEE Robotics and Au*tomation Letters, vol. 7, no. 2, pp. 2407–2414, 2022.
- [93] F. Lin, C. Bergeles, and G. Yang, "Biometry-based concentric tubes robot for vitreoretinal surgery," in 37th Annual International Conference of the IEEE Engineering in Medicine and Biology Society (EMBC), 2015, pp. 5280–5284.
- [94] T. L. Bruns, A. A. Remirez, M. A. Emerson, R. A. Lathrop, A. W. Mahoney, H. B. Gilbert, C. L. Liu, P. T. Russell, R. F. Labadie, K. D. Weaver, and I. Robert J. Webster, "A modular, multi-arm concentric tube robot system with application to transnasal surgery for orbital tumors," *The International Journal of Robotics Research*, vol. 40, no. 2-3, pp. 521–533, 2021. [Online]. Available: https://doi.org/10.1177/02783649211000074
- [95] T. K. Morimoto and A. M. Okamura, "Design of 3-D printed concentric tube robots," *IEEE Transactions on Robotics*, vol. 32, no. 6, pp. 1419– 1430, 2016.
- [96] E. Amanov, T.-D. Nguyen, and J. Burgner-Kahrs, "Additive manufacturing of patient-specific tubular continuum manipulators," in *Medical Imaging*, vol. 9415, 2015, p. 94151.
- [97] K. Picho, B. Persons, J. F. d'Almeida, N. E. Pacheco, C. Reynolds, and L. Fichera, "Multi jet fusion of nylon-12: A viable method to 3d-print concentric tube robots?" *Hamlyn Symposium* 2022, 2022. [Online]. Available: https://arxiv.org/abs/2204.00505
- [98] J. Matthey. Nitinol technical properties. (2020). [Online]. Available: https://matthey.com/en/products-and-services/ medical-components/resource-library/nitinol-technical-properties
- [99] T. Duerig, A. Pelton, and D. Stöckel, "An overview of nitinol medical applications," *Materials Science and Engineering: A*, vol. 273, pp. 149– 160, 12 1999.
- [100] N. M. Corporation, "Fep heat shrink tubing technical information," 2022. [Online]. Available: https://www.nordsonmedical.com/Components-and-Technologies/ Heat-Shrink-Tubing/FEP-Heat-Shrink-Tubing/Technical-Information/
- [101] D. Makarets, G. Noh, K. Kim, and D. Lee, "Preliminary study of utilizing plastic tubes as a component of continuum robots," in 2014 14th International Conference on Control, Automation and Systems (ICCAS 2014), 2014, pp. 217–220.
- [102] GoodFellow, "Nitinol Tube Standard Products," 2021. [Online]. Available: http://www.goodfellow.com/A/Nitinol-Tube.html
- [103] Omnexus, "Linear coefficient of thermal expansion values of several plastics," 2021. [Online]. Available: https://omnexus.specialchem.com/polymer-properties/properties/ coefficient-of-linear-thermal-expansion#PA-PC
- [104] Thomasnet, "Nitinol tubing suppliers," 2021. [Online]. Available: https://www.thomasnet.com/products/nitinol-tubing-96129895-1.html
- [105] SMST-International-Organization, "Shape memory alloy links," 2021. [Online]. Available: https://www.asminternational.org/web/smst/ shape-memory-alloys-links
- [106] M. in China, "Nitinol tube manufacturers & suppliers," 2022. [Online]. Available: https://www.made-in-china.com/manufacturers/nitinol-tube. html
- [107] A. Pelton and T. Duerig, "Shape memory alloy treatment," U.S. Patent USOO765 876OB2, Nov. 03, 1999.
- [108] A. D. Johnson, "Hyperelasticshape setting devices and fabrication methods," U.S. Patent US20110083767A1, Apr. 14, 2011.
- [109] J. F. Boylan and Z. C. Lin, "Heat treatment for cold worked ntinol to imparta shape setting capability without eventually developing stressinduced martensite," U.S. Patent US007 976 648B1, Jul. 12, 2011.
- [110] MINITUBES, "Leading custom manufacturer of high precision miniature metallic tubing, tubular parts, and assemblies." 2022. [Online]. Available: https://www.minitubes.com/products-custom-tubing/ ?tab=FABRICATION&lang=en#expertise
- [111] M. corporation, "Nitinol tube," 2022. [Online]. Available: https://www.memry.com/nitinol-tube
- [112] Nimesis, "Nimesis technology," 2021. [Online]. Available: https://www.nimesis.com/
- [113] S. Shrivastava and A. International, Medical Device Materials: Proceedings from the Materials & Processes for Medical Devices Conference 2003, 8-10 September 2003, Anaheim, California. ASM International, 2004. [Online]. Available: https://books.google.fr/books? id=6EJRAAAMAAJ

- [114] L. Wang, "Modeling and simulation of concentric and eccentric tube continuum robots," Master's thesis, *The University of Western Ontario*, 2020.
- [115] S. Russell, SMST-2000: Proceedings of the International Conference on Shape Memory and Superelastic Technologies. A S M International, 2001. [Online]. Available: https://books.google.fr/books? id=RFy0xjiR_wYC
- [116] A. Pelton, D. T, and S. D, "A guide to shape memory and superelasticity in nitinol medical devices," *Minimally invasive therapy & allied technologies : MITAT : official journal of the Society for Minimally Invasive Therapy*, vol. 13, pp. 218–21, 09 2004.
- [117] D. Kapoor, "Nitinol for medical applications: A brief introduction to the properties and processing of nickel titanium shape memory alloys and their use in stents," *Johnson Matthey Technology Review*, vol. 61, pp. 66–76, 01 2017.
- [118] B. Sun, J. Lin, and M. Fu, "Dependence of processing window and microstructural evolution on initial material state in direct electric resistance heat treatment of niti alloy," *Materials and Design*, vol. 139, pp. 549–564, 2018. [Online]. Available: https://www.sciencedirect.com/science/article/pii/S0264127517310754
- [119] S. Sabetian, "Self-collision detection and avoidance for dual-arm concentric tube robots," Master's thesis, *Institute of Biomaterials and Biomedical Engineering University of Toronto*, 2019.
- [120] Z. Mitros, "Design and modeling of multi-arm continuum robots," Doctoral dissertation, Université catholique de Louvain, January 2022.
- [121] J. Kim, T. Looi, A. Newman, and J. Drake, "Development of deployable bending wrist for minimally invasive laparoscopic endoscope," in 2020 IEEE/RSJ International Conference on Intelligent Robots and Systems (IROS), 2020, pp. 3048–3054.
- [122] M. F. Rox, D. S. Ropella, R. J. Hendrick, E. Blum, R. P. Naftel, H. C. Bow, S. D. Herrell, K. D. Weaver, L. B. Chambless, and R. J. Webster III, "Mechatronic design of a two-arm concentric tube robot system for rigid neuroendoscopy," *IEEE/ASME Transactions on Mechatronics*, vol. 25, no. 3, pp. 1432–1443, 2020.
- [123] R. Xu, "Modeling, sensorization and control of concentric-tube robots," Doctoral dissertation, The University of Western Ontario, January 2016.
- [124] E. Ayvali, C.-P. Liang, M. Ho, Y. Chen, and J. P. Desai, "Towards a discretely actuated steerable cannula for diagnostic and therapeutic procedures," *The International Journal of Robotics Research*, vol. 31, no. 5, pp. 588–603, 2012, pMID: 22639482. [Online]. Available: https://doi.org/10.1177/0278364912442429
- [125] J. Yan, J. Chen, J. Chen, W. Yan, Q. Ding, K. Yan, J. Du, C. P. Lam, G. K. C. Wong, and S. S. Cheng, "A continuum robotic cannula with tip following capability and distal dexterity for intracerebral hemorrhage evacuation," *IEEE Transactions on Biomedical Engineering*, vol. 69, no. 9, pp. 2958–2969, 2022.
- [126] J. Kim, W. Lee, S. Kang, K.-J. Cho, and C. Kim, "A needlescopic wrist mechanism with articulated motion and kinematic tractability for micro laparoscopic surgery," *IEEE/ASME Transactions on Mechatronics*, vol. 25, no. 1, pp. 229–238, 2020.
- [127] D. V. A. Nguyen, C. Girerd, Q. Boyer, P. Rougeot, O. Lehmann, L. Tavernier, J. Szewczyk, and K. Rabenorosoa, "A hybrid concentric tube robot for cholesteatoma laser surgery," *IEEE Robotics and Automation Letters*, vol. 7, no. 1, pp. 462–469, 2022.
- [128] Y. Baran, K. Rabenorosoa, G. J. Laurent, P. Rougeot, N. Andreff, and B. Tamadazte, "Preliminary results on oct-based position control of a concentric tube robot," in *IEEE/RSJ International Conference on Intelligent Robots and Systems (IROS)*, 2017, pp. 3000–3005.
- [129] A. Gao, J. P. Carey, R. J. Murphy, I. Iordachita, R. H. Taylor, and M. Armand, "Progress toward robotic surgery of the lateral skull base: Integration of a dexterous continuum manipulator and flexible ring curette," in 2016 IEEE International Conference on Robotics and Automation (ICRA), 2016, pp. 4429–4435.
- [130] G. Dwyer, "Robotic actuation for fetoscopic interventions," Doctoral dissertation, University College London, August 2020.
- [131] Z. Mitros, S. Sadati, C. Seneci, E. Bloch, K. Leibrandt, M. Khadem, L. d. Cruz, and C. Bergeles, "Optic nerve sheath fenestration with a multi-arm continuum robot," *IEEE Robotics and Automation Letters*, vol. 5, no. 3, pp. 4874–4881, 2020.
- [132] B. Qi, Z. Yu, Z. K. Varnamkhasti, Y. Zhou, and J. Sheng, "Toward a telescopic steerable robotic needle for minimally invasive tissue biopsy," *IEEE Robotics and Automation Letters*, vol. 6, no. 2, pp. 1989– 1996, 2021.
- [133] D. B. Comber, E. B. Pitt, H. B. Gilbert, M. W. Powelson, E. S. Matijevich, J. S. Neimat, R. J. Webster, and E. J. Barth, "Optimization of curvilinear needle trajectories for transforamenal hippocampotomy," *Operative Neurosurgery*, vol. 13, pp. 15 22, 2017.

- [134] M. Farooq, W. Kim, and S. Y. Ko, "A robotic suture-passing device for possible use in sils and notes," *The International Journal of Medical Robotics and Computer Assisted Surgery*, vol. 14, p. e1916, 05 2018.
- [135] M. Farooq and S. Y. Ko, "An automated extracorporeal knot-tying system using two concentric tube robotic arms for deployment through a 3-mm port," *International Journal of Control, Automation and Systems*, vol. 18, 08 2019.
- [136] H. Alfalahi, F. Renda, C. Messer, and C. Stefanini, "Exploiting the instability of eccentric tube robots for distal force control in minimally invasive cardiac ablation," *Proceedings of the Institution of Mechanical Engineers, Part C: Journal of Mechanical Engineering Science*, vol. 235, no. 23, pp. 7212–7232, 2021. [Online]. Available: https://doi.org/10.1177/09544062211007524
- [137] B. EHRAT, "Real-time control of industrial robots for shape setting nitinol rods," Master's thesis, *University of Illinois*, 2017.
- [138] E. B. Pitt, P. J. Swaney, H. B. Gilbert, Y. Chen, R. J. Webster, and E. J. Barth, "Enabling helical needle trajectories with minimal actuation: A screw-based approach to concentric tube needle deployment," 2016.
- [139] A. A. Remirez and R. J. W. III, "Endoscopes and robots for tight surgical spaces: use of precurved elastic elements to enhance curvature," in *Medical Imaging 2016: Image-Guided Procedures, Robotic Interventions, and Modeling*, R. J. W. III and Z. R. Yaniv, Eds., vol. 9786, International Society for Optics and Photonics. SPIE, 2016, p. 97860R. [Online]. Available: https://doi.org/10.1117/12.2217718
- [140] B. Hunter Bryant Gilbert, R. J. Webster III, M. Goldfarb, N. Sarkar, N. Simaan, and M. I. Miga, "Concentric Tube Robots: Design, Deployment, and Stability," *Doctoral dissertation*, *Vanderbilt University*, 2016
- [141] P. A. York, P. J. Swaney, H. B. Gilbert, and R. J. Webster, "A wrist for needle-sized surgical robots," in 2015 IEEE International Conference on Robotics and Automation (ICRA). IEEE, 2015, pp. 1776–1781.
- [142] A. Devreker and B. Rosa and A. Desjardins and E. J. Alles and L. C. Garcia-Peraza and E. Maneas and D. Stoyanov and A. L. David and T. Vercauteren and J. Deprest and S. Ourselin and D. Reynaerts and E. Vander Poorten, "Fluidic actuation for intra-operative in situ imaging," in 2015 IEEE/RSJ International Conference on Intelligent Robots and Systems (IROS), Sep. 2015, pp. 1415–1421.
- [143] Y. Chitalia and X. Wang and J. P. Desai, "Design, Modeling and Control of a 2-DoF Robotic Guidewire," in 2018 IEEE International Conference on Robotics and Automation (ICRA), May 2018, pp. 32–37.
- [144] A. N. Florea, D. S. Ropella, E. Amanov, S. D. H. III, and R. J. W. III, "Design of a modular, multi-arm concentric tube robot featuring roller gears," in *Medical Imaging 2022: Image-Guided Procedures, Robotic Interventions, and Modeling*, C. A. Linte and J. H. Siewerdsen, Eds., vol. 12034, International Society for Optics and Photonics. SPIE, 2022, pp. 37 – 42. [Online]. Available: https://doi.org/10.1117/12.2606834
- [145] P. J. Swaney, A. W. Mahoney, A. A. Remirez, E. Lamers, B. I. Hartley, R. H. Feins, R. Alterovitz, and R. J. Webster, "Tendons, concentric tubes, and a bevel tip: Three steerable robots in one transoral lung access system," *IEEE International Conference on Robotics and Automation (ICRA)*, pp. 5378–5383, 2015.
- [146] R. J. Hendrick, S. D. Herrell, and R. J. Webster, "A multi-arm handheld robotic system for transurethral laser prostate surgery," in *IEEE International Conference on Robotics and Automation (ICRA)*, 2014, pp. 2850–2855.
- [147] P. J. Swaney, J. M. Croom, J. Burgner, H. B. Gilbert, D. C. Rucker, R. J. Webster III, K. D. Weaver, and P. T. Russell III, "Design of a quadramanual robot for single-nostril skull base surgery," in *Dynamic* Systems and Control Conference, vol. 45318, 2012, pp. 387–393.
- [148] S. Esakkiappan, B. Shirinzadeh, and W. Wei, "Development of a cost-effective actuation unit for three DOF concentric tube robot in minimally invasive surgery," *IEEE/ASME International Conference on Advanced Intelligent Mechatronics*, AIM, vol. 2019-July, pp. 1013– 1018, 2019.
- [149] R. Xu, "Modeling , Sensorization and Control of Concentric-Tube Robots," Doctoral dissertation, The University of Western Ontario, 2017
- [150] C. Girerd and T. K. Morimoto, "Design and Control of a Hand-Held Concentric Tube Robot for Minimally Invasive Surgery," *IEEE Transactions on Robotics*, pp. 1–17, 2020.
- [151] H. Su, G. Li, D. C. Rucker, R. J. Webster, and G. S. Fischer, "A Concentric Tube Continuum Robot with Piezoelectric Actuation for MRI-Guided Closed-Loop Targeting," *Annals of Biomedical Engineering*, vol. 44, no. 10, pp. 2863–2873, 2016.

- [152] D. C. Rucker, B. A. Jones, and R. J. Webster III, "A geometrically exact model for externally loaded concentric-tube continuum robots," *IEEE Transactions on Robotics*, vol. 26, no. 5, pp. 769–780, 2010.
- [153] M. Boushaki, C. Liu, B. Herman, V. Trevillot, M. Akkari, and P. Poignet, "Optimization of concentric-tube robot design for deep anterior brain tumor surgery," in 2016 14th International Conference on Control, Automation, Robotics and Vision (ICARCV), 2016, pp. 1–6.
- [154] C. M. Graves, A. Slocum, R. Gupta, and C. J. Walsh, "Towards a compact robotically steerable thermal ablation probe," in *IEEE International Conference on Robotics and Automation*, 2012, pp. 709–714.
- [155] J. Burgner, P. J. Swaney, T. L. Bruns, M. S. Clark, D. C. Rucker, E. C. Burdette, and R. J. Webster, "An Autoclavable Steerable Cannula Manual Deployment Device: Design and Accuracy Analysis," *Journal* of Medical Devices, Transactions of the ASME, vol. 6, no. 4, pp. 1–7, 2012
- [156] J. Burgner, D. C. Rucker, H. B. Gilbert, P. J. Swaney, P. T. Russell, K. D. Weaver, and R. J. Webster, "A telerobotic system for transnasal surgery," *IEEE/ASME Transactions on Mechatronics*, vol. 19, no. 3, pp. 996–1006, 2014.
- [157] J. Wang, X. Yang, P. Li, S. Song, L. Liu, and M. Q. Meng, "Design of a multi-arm concentric-tube robot system for transnasal surgery," *Medical and Biological Engineering and Computing*, vol. 58, no. 3, pp. 497–508, 2020.
- [158] H. Yu, L. Wu, K. Wu, and H. Ren, "Development of a Multi-Channel Concentric Tube Robotic System with Active Vision for Transnasal Nasopharyngeal Carcinoma Procedures," *IEEE Robotics* and Automation Letters, vol. 1, no. 2, pp. 1172–1178, 2016.
- [159] N. V. Vasilyev, A. H. Gosline, A. Veeramani, M. T. Wu, G. P. Schmitz, R. T. Chen, V. Arabagi, P. J. del Nido, and P. E. Dupont, "Tissue removal inside the beating heart using a robotically delivered metal mems tool," *The International Journal of Robotics Research*, vol. 34, no. 2, pp. 236–247, 2015.
- [160] P. Swaney, P. York, H. Gilbert, J. Burgner-Kahrs, and R. Webster, "Design, fabrication, and testing of a needle-sized wrist for surgical instruments," *Journal of Medical Devices*, vol. 11, 09 2016.
- [161] A. B. Prasai, A. Jaiprakash, A. K. Pandey, R. Crawford, J. Roberts, and L. Wu, "Design and fabrication of a disposable micro end effector for concentric tube robots," in 14th International Conference on Control, Automation, Robotics and Vision (ICARCV), 2016, pp. 1–6.
- [162] C. Girerd, A. V. Kudryavtsev, P. Rougeot, P. Renaud, K. Rabenorosoa, and B. Tamadazte, "Slam-based follow-the-leader deployment of concentric tube robots," *IEEE Robotics and Automation Letters*, vol. 5, no. 2, pp. 548–555, 2020.
- [163] P. Dupont, "Concentric Tube Robot Chicken Leg Dissection," Sep 23,2016. [Online]. Available: https://www.youtube.com/watch?v= pX-WLbMPJTY
- [164] I. S. Godage, A. A. Remirez, R. Wirz, K. D. Weaver, J. Burgner-Kahrs, and R. J. Webster, "Robotic intracerebral hemorrhage evacuation: An in-scanner approach with concentric tube robots," in 2015 IEEE/RSJ International Conference on Intelligent Robots and Systems (IROS), 2015, pp. 1447–1452.
- [165] J. Granna, A. Nabavi, and J. Burgner-Kahrs, "Computer-assisted planning for a concentric tube robotic system in neurosurgery," *Interna*tional Journal of Computer Assisted Radiology and Surgery, vol. 14, 11 2018.
- [166] K. Eastwood, P. Francis, H. Azimian, A. Swarup, T. Looi, J. Drake, and H. Naguib, "Design of a contact-aided compliant notched-tube joint for surgical manipulation in confined workspaces," *Journal of Mechanisms* and Robotics, vol. 10, 10 2017.
- [167] R. M. Grassmann, S. Lilge, P. H. U. Le, and J. Burgner-kahrs, "CTCR Prototype Development: An Obstacle in the Research Community?" RSS 2020 Robotics Retrospectives Workshop, 2020.
- [168] virtuososurgical, "virtuoso surgical," 2022. [Online]. Available: https://virtuososurgical.net/history/
- [169] P. E. Dupont, B. J. Nelson, M. Goldfarb, B. Hannaford, A. Menciassi, M. K. O'Malley, N. Simaan, P. Valdastri, and G.-Z. Yang, "A decade retrospective of medical robotics research from 2010 to 2020," *Science Robotics*, vol. 6, no. 60, p. eabi8017, 2021. [Online]. Available: https://www.science.org/doi/abs/10.1126/scirobotics.abi8017
- [170] R. H. Taylor, N. Simaan, A. Menciassi, and G.-Z. Yang, "Surgical robotics and computer-integrated interventional medicine," *Proceedings* of the IEEE, vol. 110, no. 7, pp. 823–834, 2022.



Chibundo J. Nwafor received a B.Eng. in Electrical/Electronics from Anambra State University, Uli, Nigeria, in 2012 and a Master Degree on Control for Green Mechatronics from Université Bourgogne Franche-Comté (UBFC), Besançon, France, in 2019. He is currently pursuing his PhD degree in Robotics at UBFC and a member of the Automatic Control and Micro-Mechatronic Systems Department of FEMTO-ST Institute. His research interest include continuum robotics and micro-mechatronics systems for biomedical applications.



2022.

Tania K. Morimoto received the B.S. degree from Massachusetts Institute of Technology, Cambridge, MA, in 2012 and the M.S. and Ph.D. degrees from Stanford University, Stanford, CA, in 2015 and 2017, respectively, all in mechanical engineering. She is currently an Assistant Professor of mechanical and aerospace engineering and an Assistant Professor of surgery with University of California, San Diego. Her research interests include robotics, haptics, and engineering education. Dr. Morimoto was the recipient of the NSF CARRER Award in



Cédric Girerd received an Engineering degree in Mechatronics from SIGMA Clermont and a Master of Science in Robotics from University Blaise Pascal in Clermont-Ferrand, France, both in 2014. He also received a Ph.D. degree in Robotics from the University of Strasbourg, France, in 2018. He then worked as a Postdoctoral Scholar at the FEMTO-ST Institute in France for one year and at UCSD for three years. Since February 2022, he is a full-time CNRS Researcher in France, and a Visiting Scholar at UCSD. His research focuses on the design and

control of continuum and soft robots.



Kanty Rabenorosoa received the M.S. degree in electrical engineering from Institut National des Sciences Appliquées in Strasbourg, France, in 2007, and the Ph.D. degree in automatic control from the University of Franche-Comté, Besançon, France, in 2010. He was a Post-Doctoral Fellow at Laboratoire d'Informatique, de Robotique et de Microélectronique de Montpellier, University of Montpellier, France, from 2011 to 2012. He is currently an Associate Professor at the National School of Mechanics and Microtechnologies (ENSMM) and

affiliated to AS2M Department, FEMTO-ST Institute, Besançon. His research interests include mechatronics, smart actuators, soft and continuum robotics for medical applications.



Guillaume J. Laurent received his Ph.D. in control systems and computer sciences from the University of Franche-Comté in France, in 2002. He is currently associate professor at the National School of Mechanics and Microtechnologies (ENSMM) in Besançon. He is member of the Automatic Control and Micro-Mechatronic Systems Department of FEMTO-ST Institute. His research interests include microrobotics, computer vision, parallel and continuum robots.